

Rectangular polar quadrature in 1D and its error analysis

Krishna Yamanappa Poojara ^{*} Sabhrant Sachan[†] Ambuj Pandey [‡]

Preliminary draft

Abstract

This paper presents a one-dimensional analog of the Rectangular-Polar (RP) integration strategy [2] and its convergence analysis for weakly singular convolution integrals. The key idea of this method is to break the whole integral into integral over non-overlapping patches (subdomains) and achieve convergence by increasing the number of patches while approximating the integral on patches accurately using a fixed number of quadrature points. The non-singular integrals are approximated to high-order using Fejér first quadrature, and a specialized integration strategy is designed and incorporated for singular integrals where the kernel singularity is resolved by mean of Polynomial Change of Variable (PCV). We prove that for high-order convergence, it is essential to compute integral weights accurately, and the method's convergence rate depends critically on the degree of the PCV and the singularity of the integral kernel. Specifically, for kernels of the form $|x - y|^{-\alpha}$ ($\alpha > -1$), the method achieves high-order convergence if and only if $p(1 - \alpha) \in \mathbb{N}$. This relationship, first observed numerically in [4], highlights the importance of choosing an appropriate degree p for the PCV. A new error estimate in a framework where convergence is achieved by reducing the approximating domain size while keeping the number of discretization points fixed is derived for the Fejér first quadrature, decay rate of Chebyshev coefficients, and the error in approximating continuous Chebyshev coefficients with discrete ones. Numerical experiments corroborate the theoretical findings, showcasing the effectiveness of the RP strategy for accurately solving singular integral equations. As an application of the method, numerical solutions of the surface scattering problem in the two dimensions are computed for complex domains, and the algorithm's efficacy is demonstrated for large-scale problems.

1 Introduction

Recently, an efficient high-order Rectangular-Polar (RP) integration strategy was introduced in [2] for the approximation of weakly singular convolution integrals which appear in the context of surface scattering problems in three dimensions. In [2], the authors demonstrated the spectral accuracy of the RP integration strategy through several numerical experiments and simulated scattering phenomena on complex geometries relevant to real-world applications. Due to its ability to handle singular kernels with high-order accuracy, even for complex geometric domains, the RP strategy has been successfully applied to various practical problems in science and engineering [21, 16, 10, 9, 11]. The hallmark of the RP integration scheme's high accuracy lies in its design and the specialized quadrature rules it employs for the evaluation of singular integrals. These rules leverage a Polynomial Change of Variable (PCV), which clusters nearly half of the integration nodes near the singular points, thereby regularizing the kernel. While the high-order convergence of the RP quadrature scheme has been demonstrated in numerous applications [11, 3, 16], rigorous convergence analysis of the method is, to the best of our knowledge, not yet reported in the

^{*}Computing and Mathematical Sciences, Caltech, Pasadena, CA 91125, USA, kyp6174@caltech.edu

[†]Computing and Mathematical Sciences, Caltech, Pasadena, CA 91125, USA, ssachan@caltech.edu

[‡]Indian Institute of Science Education and Research Bhopal (IISER Bhopal), ambuj@iiserb.ac.in

literature. In this paper, we present a rigorous quadrature analysis of a one-dimensional analog of the RP integration scheme for the evaluation of convolution integral operators of the form:

$$\mathcal{K}[u](x) := \int_{\Omega} g_{\alpha}(|x - y|) u(y) dy, \quad x \in \Omega, \quad (1)$$

where Ω is a closed, bounded interval in \mathbb{R} , and u denotes an integral density assumed to belong to the function space $X^m(\Omega) = C^m(\Omega) \cap C_{pw}^{m+2}(\Omega)$, implying u is m -times continuously differentiable with piecewise continuous $(m + 2)$ -th derivatives. The kernel $g_{\alpha}(|x - y|)$ takes the form:

$$g_{\alpha}(|x - y|) := \begin{cases} |x - y|^{-\alpha}, & 0 < \alpha < 1, \\ \log|x - y|, & \alpha = 0. \end{cases} \quad (2)$$

This analysis is critical for selecting key algorithmic parameters that influence the high-order accuracy of the methodology and its extension to higher dimensions. For example, in [4], the authors computationally observed that, unlike the logarithmic kernel, the RP strategy does not exhibit high-order convergence for kernels of the form $|x - y|^{-\alpha}$ for all polynomial degrees in the PCV. Specifically, they noted that for kernels of the form $g_{\alpha}(x, y) = |x - y|^{-\alpha}$ with $0 < \alpha < 1$, the convergence rate depends on the degree p of the polynomial in the PCV, achieving high-order convergence only for specific values of p . Empirical evidence suggests that high-order convergence occurs when $p(1 - \alpha) \in \mathbb{N}$. This raises an important question: *for a given α and density regularity m , what values of p ensure high-order convergence of the RP quadrature?* We answer this question (see Section 4, Theorem 4.9, and Theorem 4.11) and rigorously prove that the RP method achieves high-order convergence if and only if $p(1 - \alpha) \in \mathbb{N}$. In such cases, the precise order of convergence is $m + 2 - \alpha$. When $p(1 - \alpha) \notin \mathbb{N}$, the convergence order is limited to $\min\{m + 2 - \alpha, 2p(1 - \alpha)\}$. For infinitely smooth u , the scheme achieves exponential convergence if $p(1 - \alpha) \in \mathbb{N}$, while otherwise, the convergence rate is restricted to $2p(1 - \alpha)$. These theoretical results are corroborated by extensive computational experiments, showing close agreement between theoretical and computational convergence rates.

To improve computational efficiency, the RP strategy [2] divides the integration domain into non-overlapping subdomains (patches), approximating the integral on each patch with a high-order quadrature rule using a fixed number of nodes. High-order convergence is achieved by increasing the number of patches while keeping the number of nodes on each patch constant. However, a rigorous error analysis of this approach requires results on the following for functions $f \in X^m[a, b]$ as a function of the interval length $h = b - a$:

1. Error in Fejér first quadrature.
2. Decay rate of Chebyshev coefficients of f .
3. Truncation error in approximating f by its Chebyshev series.
4. Error in approximating continuous Chebyshev coefficients with discrete coefficients.

While these results are well-established for fixed h as $n \rightarrow \infty$, they are not explicitly available for the case where convergence is achieved by shrinking h while keeping n fixed. In this paper, we derive explicit error estimates for both cases, making our results applicable to various computational techniques where convergence is achieved by domain decomposition, such as hp -Finite Element and Spectral Element Methods. As mentioned in [2, cf. Section 5.1], our analysis also demonstrates the necessity of accurate singular integral weights for high-order convergence. If singular weights are computed inaccurately, the asymptotic convergence rate drops to $O(h)$ for logarithmic kernels and $O(h^{1-\alpha})$ for α -kernels. However, numerical experiments indicate that 24–32 nodes per patch with appropriate p are sufficient for accurate weight computation, mitigating this issue. Finally, we make an important observation regarding singularity

treatment. Breaking the singular integral at the singularity point improves the convergence rate by two orders compared to treating it without subdivision. This insight underscores the importance of specialized singularity handling in achieving high accuracy with the RP strategy.

The proposed one-dimensional RP-Integration scheme offers additional computational advantages over a higher-dimensional version. For instance, unlike the three-dimensional approach [2] where singular integral weights require $O(P_{\text{near}}N)$ memory, in the one dimension, it needs only $O(1)$ memory for the weight storage, where N is the number of unknowns and P_{near} is the number of near singular patch. Thus, the proposed one-dimensional RP integration scheme can efficiently evaluate convolution integrals of the form 1 with high-order accuracy. For the N-point discretization problem, our convolution computation needs $O(N^2)$ operations. However, this process can be significantly sped up using existing fast summation methods such as the Fast Multipole Method [14], and the sum of exponential approximation [22] to name a few.

The proposed method can be straightforwardly adopted as a Nyström solver for an accurate numerical solution of integral equations in one dimension. For instance, in [3] the RP strategy is incorporated for the solution of the second kind Fredholm equation over the boundary of square domain. Moreover, the applicability of the RP strategy can be easily extended for the boundary of complicated domains and to illustrate this, in Section 6, we have implemented the proposed method for the solution of two-dimensional surface scattering by acoustic waves. We have simulated the aforementioned scattering problem by employing the proposed method to the second kind equivalent integral equation and the resulting linear system is solved iteratively by means of the generalized minimal residual method (GMRES). Unlike the Finite Element and Finite Difference method, our solver is dispersion less and capable of solving a large-scale problem accurately.

The rest of the paper is organized as follows. In Section 2 we present the details of the proposed quadrature which comprises of decomposition of the domain into non-overlapping patches, treatment of regular, singular, and near-singular integrals, and the implementation of the change of variable. Section 3 presents new error bounds on Chebyshev coefficients related to Chebyshev polynomials of the first kind in terms of varying patch length and index of the coefficient, from which we have also derived a novel error bound on Fejér quadrature. Section 4 presents the error analysis of the proposed numerical integration method. Section 5 demonstrates a variety of numerical examples, which align with the error analysis. To demonstrate the applicability of our method, in Section 6 we have also included simulation results for the two-dimensional surface scattering problems. We concluded the paper with comments on possible directions for future work.

2 Methodology

In this section, we describe the proposed integration scheme for an accurate evaluation of integral operator

$$\mathcal{K}[u](x) := \int_{\Omega} g_{\alpha}(|x-y|) u(y) dy, \text{ for } x \in \Omega, \quad (3)$$

where Ω is a closed bounded interval in \mathbb{R} , and the integral density $u \in X^m(\Omega)$, $m \geq 0$. We also assume that the integral kernel $g_{\alpha}(|x-y|)$ is a weakly singular, that is, $g_{\alpha}(|x-y|)$ is continuous for all $x, y \in \Omega$, $x \neq y$, and there exist a positive constant C such that

$$|g_{\alpha}(|x-y|)| \leq C|x-y|^{-\alpha}, \quad x, y \in \Omega, x \neq y, \quad (4)$$

for $0 < \alpha < 1$. Owing to the kernel singularity in equation (3) a straightforward application of the high-order quadrature rule exhibits low order convergence, and hence a specialized quadrature rule must be designed and used if high-order accuracy is desired. In order to deal with the singular character of the

kernel efficiently, we utilize a strategy based on local parametrization that we explain in what follows. To this end, we start by representing Ω as a union of P patches namely $\Omega_1, \Omega_2, \dots, \Omega_P$ such that

$$\Omega = \bigcup_{\ell=1}^P \bar{\Omega}_\ell, \quad \text{and } \Omega_\ell \cap \Omega_q = \emptyset \text{ for } \ell \neq q, \quad (5)$$

where each $\bar{\Omega}_\ell$ (closure of Ω_ℓ) is an image of the closed set $[-1, 1]$ via a smooth invertible parametrization ξ_ℓ . Using this patching decomposition and parametrization, integral (3) can be re-written as

$$\mathcal{K}[u](x) = \sum_{\ell=1}^P \mathcal{K}_\ell[u](x), \quad (6)$$

where

$$\mathcal{K}_\ell[u](x) = \int_{-1}^1 g_\alpha(|x - \xi_\ell(t)|) u(\xi_\ell(t)) J_\ell(t) dt, \quad (7)$$

and $J_\ell(t)$ denote the Jacobian of parametrization ξ_ℓ . Note that a high-order approximation of integral (7) depends on the position of target point x with respect to the integration patch Ω_ℓ . For instance, if the target point x lies in the integration patch Ω_ℓ or very close to Ω_ℓ then the integrand in (7) becomes singular or near singular respectively. Thus, depending upon the location of x relative to the integration patch Ω_ℓ , we partition the set of integral in (6) into three different classes, namely, regular integral, singular integral and near singular integral.

In the case of regular integral, target point x is sufficiently away from the integration patch Ω_ℓ , so the integrand in (7) becomes smooth (as the integral kernel is smooth), and high-order accuracy can be achieved by utilizing any of the classical high-order quadrature rules. For instance, in our implementations, to evaluate the integral (7) we have used the FF-Rule, discussed in [7] and achieved high-order convergence. To be precise, if x is sufficiently away from Ω_ℓ , then the discrete operator

$$\mathcal{K}_{\ell, \text{reg}}^n[u](x) = \sum_{i=0}^{n-1} w_i g_\alpha(|x - \xi_\ell(t_i)|) u(\xi_\ell(t_i)) J_\ell(t_i), \quad (8)$$

yields high-order approximation to the equation (7), where $t_i = \cos\left(\pi \frac{2i+1}{2n}\right)$ denotes the open Chebyshev nodes in the interval $[-1, 1]$ and w_i denotes the weights for the FF-Rule [7], given by

$$w_i = \frac{2}{n} \left(1 - 2 \sum_{k=0}^{\lfloor \frac{n}{2} \rfloor} \frac{\cos(kv_{2i+1})}{4k^2 - 1} \right), \quad v_{2i+1} = \frac{(2i+1)\pi}{n}. \quad (9)$$

We discuss the convergence of FF-Rule in Theorem 3.8, which illustrates order of convergence of this quadrature in terms of the decay rate of Chebyshev coefficients of the function. The central focus of our presentation lies in the treatment of singular integral and its convergence analysis, which arises when the target point x lies in the integration patch Ω_ℓ . To circumvent the kernel singularity in g_α at $x = y$, we utilize local Chebyshev expansion of the integral density and a local change of variable that we describe in what follows. The truncated Chebyshev expansion of integral density $\phi_\ell(t) = u(\xi_\ell(t)) J_\ell(t)$ in the patch Ω_ℓ can be obtained as

$$\phi_\ell(t) \approx \sum_{k=0}^{n-1} \tilde{c}_k^\ell T_k(t), \quad (10)$$

where T_k denotes the Chebyshev polynomial of the first kind of degree k [15], and \tilde{c}_k^ℓ is the discrete Chebyshev coefficient of ϕ_ℓ that can be computed as

$$\tilde{c}_k^\ell = \frac{\gamma_k}{n} \sum_{i=0}^{n-1} \phi_\ell(t_i) T_k(t_i), \text{ with } \gamma_k = \begin{cases} 1, & \text{if } k = 0 \\ 2, & \text{otherwise.} \end{cases} \quad (11)$$

Note that, the coefficients \tilde{c}_k^ℓ , for all $k = 0, 1, \dots, n-1$, and for all $\ell = 1, 2, \dots, P$, can be computed in $O(nP \log n)$ operations using the FFT. Now using discrete Chebyshev series (10), integral (7) can be approximated as

$$\mathcal{K}_\ell[u](x) \approx \mathcal{K}_\ell^n[u](x) = \sum_{k=0}^{n-1} \tilde{c}_k^\ell \beta_k^\ell(x), \text{ where } \beta_k^\ell(x) = \int_{-1}^1 g_\alpha(|x - \xi_\ell(t)|) T_k(t) dt. \quad (12)$$

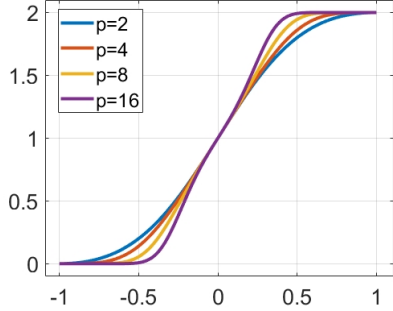
Note that the integrand in $\beta_k^\ell(x)$ is singular at $x = \xi_\ell(t)$ and hence special care is required for its accurate approximation. To compute $\beta_k^\ell(x)$ with high degree of precision, we have employed a change of variable technique similar to those utilized in [2]. Therefore, we now employ the change of variable ψ_p which smoothens the integrand at the edges as discussed in [2, 12] to handle the singularity in the integral $\beta_k^\ell(x)$, which is defined below for $p \geq 2$,

$$\psi_p(t) = 2 \frac{[v_p(t)]^p}{[v_p(t)]^p + [v_p(-t)]^p}, \quad (13)$$

and

$$v_p(t) = \left(\frac{1}{2} - \frac{1}{p} \right) t^3 + \frac{t}{p} + \frac{1}{2}, \quad -1 \leq t \leq 1. \quad (14)$$

There are two approaches to apply this change of variable: one to overcome the singularity within the interior of the domain and the other to address the singularity at the edges. Upon implementing both approaches we observed a peculiar behavior in the convergence order, which we demonstrate in the table below. As illustrated above, the change of variable method addressing the singularity at the edges shows



n	boundary		interior	
	error	order	error	order
4	2.46e-02	-	2.75e-01	-
8	2.98e-05	9.69	1.33e-02	4.37
16	1.65e-07	7.50	3.02e-05	8.78
32	7.27e-14	21.1	5.58e-08	9.08
64	-	-	7.10e-10	6.30
128	-	-	9.28e-12	6.26
256	-	-	1.19e-13	6.29
512	-	-	3.00e-15	5.31
1024	-	-	2.00e-16	3.91

Figure 1: The change of variable function ψ_p is plotted for various values of p , we can see the higher order derivatives of ψ_p vanishes at the edges as p increases. The table in right demonstrates behavior of the polynomial change of variable [2, equation (40)], which is implemented for the function $|t|^{-0.1}$ on $[-1, 1]$ at the singularity $t = 0$ on boundary and interior with $p = 7$. We refer [13, Theorem 2] for theoretical justification.

superior convergence compared to the one focusing on the interior singularity. Consequently, we split the integral in equation (12) at the singular point $t_x := \xi_\ell^{-1}(x)$ into two parts: $\beta_k^\ell(x) = \beta_{k,L}^\ell(x) + \beta_{k,R}^\ell(x)$, where

$$\beta_{k,L}^\ell(x) = \int_{-1}^{t_x} g_\alpha(|x - \xi_\ell(t)|) T_k(t) dt, \text{ and } \beta_{k,R}^\ell(x) = \int_{t_x}^1 g_\alpha(|x - \xi_\ell(t)|) T_k(t) dt. \quad (15)$$

After utilizing the change of variable (13), we approximate $\beta_{k,L}^\ell, \beta_{k,R}^\ell$ by FF-Rule, and denote the approximations as $\tilde{\beta}_{k,L}^\ell$ and $\tilde{\beta}_{k,R}^\ell$ respectively. Finally, we conclude our singular integration scheme by introducing the singular integral operator $\mathcal{K}_{\ell,\text{sing}}^n[u](x)$,

$$\mathcal{K}_\ell^n[u](x) \approx \mathcal{K}_{\ell,\text{sing}}^n[u](x) = \sum_{k=0}^{n-1} \tilde{c}_k^\ell(\phi_\ell) \tilde{\beta}_k^\ell(x), \quad \tilde{\beta}_k^\ell = \tilde{\beta}_{k,L}^\ell + \tilde{\beta}_{k,R}^\ell. \quad (16)$$

The only case which remains to be dealt with is near singular integration, in which the target point is close to the integration patch such that a direct application of the FF-Rule exhibits poor convergence due to the presence of the weakly singular kernel. Although the kernel remains finite in this case, it can blow up to significantly larger values, creating numerical challenges. We follow two fold strategy to overcome the near singularity phenomenon. First, we project t_x (see (15)) to the nearest edge of the parametric space corresponding to the integration patch. Then, we follow the singular integration scheme discussed above for the projected point.

3 Chebyshev Coefficients: Decay with Interval Size

Throughout this paper, the symbol C stands for a positive constant taking on different values on different occurrences. In this section, we will discuss the decay of the Chebyshev coefficients which incorporates length of the interval as it play a major role in deriving convergence rates of our methodology. In literature, many authors have discussed the convergence of Chebyshev coefficients [20, 19, 18, 17], however, in best of our knowledge, the decay rate in terms of the length of the interval are not reported. We now investigate the convergence rates of coefficients with size of the patch and index. Throughout this section, let $\Omega = [a, b]$, $h = b - a$ and define c_k as the Chebyshev coefficients of the function \tilde{u} , where

$$\tilde{u}(t) = u(\xi(t)), \quad \xi(t) = \frac{h}{2}t + \frac{a+b}{2}, \quad -1 \leq t \leq 1. \quad (17)$$

The function \tilde{u} is simply a re-parametrization of u on the interval Ω to $[-1, 1]$. We aim to estimate c_k in terms of the patch length h and coefficient index k , to this end, we begin with a preliminary lemma showing the behavior of the coefficients as h tends to zero.

Lemma 3.1. *Let u be a continuous function on Ω , $x_0 = \frac{a+b}{2}$ and $k \geq 1$. If a, b are bounded as h tends to zero, then the Chebyshev coefficients c_k of \tilde{u} satisfy*

$$c_0 \rightarrow u(x_0), \quad c_k \rightarrow 0, \quad \text{as } h \rightarrow 0.$$

Proof. For $k \geq 1$,

$$c_k = \frac{2}{\pi} \int_{-1}^1 \tilde{u}(t) \frac{T_k(t)}{\sqrt{1-t^2}} dt = \frac{2}{\pi} \int_0^\pi \tilde{u}(\cos \theta) \cos(k\theta) d\theta.$$

Using Dominated convergence theorem,

$$\lim_{h \rightarrow 0} c_k = \frac{2}{\pi} \int_0^\pi \lim_{h \rightarrow 0} \tilde{u}(\cos \theta) \cos(k\theta) d\theta = \frac{2}{\pi} u(x_0) \int_0^\pi \cos(k\theta) d\theta = 0.$$

Similarly, the result follows for $k = 0$. □

To understand how fast Chebyshev coefficients c_k converge to zero for $k \geq 1$, we use integration by parts. We obtain

$$c_k = \frac{1}{\pi} \int_{-\pi}^\pi \tilde{u}(\cos \theta) \cos(k\theta) d\theta = \frac{h}{2k} \frac{1}{\pi} \int_{-\pi}^\pi \tilde{u}'(\cos \theta) \sin(\theta) \sin(k\theta) d\theta. \quad (18)$$

To simplify calculations, define

$$I_M[\tilde{u}^{(i)}, j, k] = \int_{-\pi}^{\pi} \tilde{u}^{(i)}(\cos \theta) \sin^j(\theta) \cos^{i-j}(\theta) \zeta_M(k\theta) d\theta, \quad (19)$$

where i, M are non-negative integers, and j is an integer such that $j \leq i$. If $j < 0$, then define $I_M[\tilde{u}^{(i)}, j, k] = 0$. Here M corresponds to the number of times integration by parts is performed and $\zeta_M(\theta) = \cos \theta$ if M is even, else $\zeta_M(\theta) = \sin \theta$; $\tilde{u}^{(i)}$ corresponds to i -th derivative of \tilde{u} , where i depends on the regularity of \tilde{u} . Before formulating an expression for the coefficients c_k , we describe a recursive relation which plays a crucial rule in obtaining a bound for c_k .

Lemma 3.2. *If $u \in X^m(\Omega)$ then for integers i, j, M with $0 \leq j \leq i \leq m$, $M \geq 0$ and $k \in \mathbb{N}$, $I_M[\tilde{u}^{(i)}, j, k]$ satisfies the following recursive relation*

$$I_M[\tilde{u}^{(i)}, j, k] = \frac{(-1)^M}{k} \left(-j I_{M+1}[\tilde{u}^{(i)}, j-1, k] + (i-j) I_{M+1}[\tilde{u}^{(i)}, j+1, k] + \frac{h}{2} I_{M+1}[\tilde{u}^{(i+1)}, j+1, k] \right). \quad (20)$$

Additionally, if $u \in C^{m+2}(\Omega)$ then equation (20) holds for $0 \leq j \leq i \leq m+1$.

Proof. Using integration by parts, and the relation

$$\int \zeta_M(k\theta) d\theta = \frac{(-1)^M}{k} \zeta_{M+1}(k\theta),$$

for $0 \leq i \leq m-1$, $I_M[\tilde{u}^{(i)}, j, k]$ can be written as

$$I_M[\tilde{u}^{(i)}, j, k] = \int_{-\pi}^{\pi} \tilde{u}^{(i)}(\cos \theta) \sin^j(\theta) \cos^{i-j}(\theta) \zeta_M(k\theta) d\theta \quad (21)$$

$$\begin{aligned} &= \frac{(-1)^M}{k} \frac{h}{2} \int_{-\pi}^{\pi} \tilde{u}^{(i+1)}(\cos \theta) \sin^{j+1}(\theta) \cos^{i-j}(\theta) \zeta_{M+1}(k\theta) d\theta \\ &+ \frac{(-1)^{M+1} j}{k} \int_{-\pi}^{\pi} \tilde{u}^{(i)}(\cos \theta) \sin^{j-1}(\theta) \cos^{i-(j-1)}(\theta) \zeta_{M+1}(k\theta) d\theta \\ &+ \frac{(-1)^M}{k} (i-j) \int_{-\pi}^{\pi} \tilde{u}^{(i)}(\cos \theta) \sin^{j+1}(\theta) \cos^{i-(j+1)}(\theta) \zeta_{M+1}(k\theta) d\theta. \end{aligned} \quad (22)$$

Hence, for $u \in X^m(\Omega)$ we have the following recurrence relation for $1 \leq i \leq m-1$,

$$I_M[\tilde{u}^{(i)}, j, k] = \frac{(-1)^M}{k} \left(-j I_{M+1}[\tilde{u}^{(i)}, j-1, k] + (i-j) I_{M+1}[\tilde{u}^{(i)}, j+1, k] + \frac{h}{2} I_{M+1}[\tilde{u}^{(i+1)}, j+1, k] \right). \quad (23)$$

Since $u^{(m)}$ is not differentiable in Ω and $\tilde{u}(\cos(\cdot)) \in C_{\text{pw}}^{m+2}[-\pi, \pi]$, there exist discontinuities $\{s_\ell\}_{\ell=0}^{n_d}$ of $(m+1)$ -th derivative of $\tilde{u}(\cos \theta)$ for some $n_d \in \mathbb{N}$ such that $[-\pi, \pi] = \cup_{\ell=1}^{n_d} [s_{\ell-1}, s_\ell]$. Therefore, $\tilde{u}(\cos(\cdot)) \in C^{m+2}(s_{\ell-1}, s_\ell)$ for each ℓ . Using this decomposition, an application of integration by parts one more time gives

$$\begin{aligned} I_M[\tilde{u}^{(m)}, j, k] &= \int_{-\pi}^{\pi} \tilde{u}^{(m)}(\cos \theta) \sin^j(\theta) \cos^{i-j}(\theta) \zeta_m(k\theta) d\theta \\ &= \frac{(-1)^m}{k} \sum_{\ell=1}^{n_d} \left[\left(\tilde{u}^{(m)}(\cos \theta) \sin^j(\theta) \cos^{i-j}(\theta) \zeta_{m+1}(k\theta) \right)_{s_{\ell-1}}^{s_\ell} \right. \\ &\quad \left. - \int_{s_{\ell-1}}^{s_\ell} \left(\tilde{u}^{(m)}(\cos \theta) \sin^j(\theta) \cos^{i-j}(\theta) \right)' \zeta_{m+1}(k\theta) d\theta \right]. \end{aligned} \quad (24)$$

Using continuity of $u^{(m)}$, the first term in (24) is zero. Since the discontinuities of $\tilde{u}^{(m+1)}$ are finitely many, the second term in (24) can be simplified as

$$\sum_{\ell=1}^{n_d} \int_{s_{\ell-1}}^{s_\ell} \left(\tilde{u}^{(m)}(\cos \theta) \sin^j(\theta) \cos^{i-j}(\theta) \right)' \zeta_{m+1}(k\theta) d\theta = \int_{-\pi}^{\pi} \left(\tilde{u}^{(m)}(\cos \theta) \sin^j(\theta) \cos^{i-j}(\theta) \right)' \zeta_{m+1}(k\theta) d\theta.$$

This implies that we obtained the same recursive relation in this case. Additionally, if $u \in C^{m+2}(\Omega)$, it is easy to see that equation (23) holds even for $0 \leq i \leq m+1$ as the step (21) is valid. \square

Now, using (19), c_k in (18) can be re-expressed as $c_k = \frac{1}{2\pi} \frac{h}{k} I_1[\tilde{u}^{(1)}, 1, k]$. Performing integration by parts iteratively M times provides the following lemma.

Lemma 3.3. *Let $u \in X^m(\Omega)$ and $1 \leq M \leq m+1$, $k \in \mathbb{N}$, then*

$$c_k = \sum_{i=1}^M \sum_{j=0}^i \frac{h^i}{k^M} \alpha_{ij}^{(M)} I_M[\tilde{u}^{(i)}, j, k], \quad (25)$$

where $\alpha_{ij}^{(M)}$ are constants defined recursively and independent of k and h , that is, for $0 \leq j \leq i$, $1 \leq i \leq M$,

$$\alpha_{ij}^{(M)} = \alpha_{1,ij}^{(M)} + \alpha_{2,ij}^{(M)} + \alpha_{3,ij}^{(M)}, \quad \text{where } \alpha_{1,ij}^{(M)} = \begin{cases} 0, & \text{if } i = M \text{ or } j = i \\ (-1)^M (j+1) \alpha_{i(j+1)}^{(M-1)}, & \text{otherwise,} \end{cases}$$

$$\alpha_{2,ij}^{(M)} = \begin{cases} 0, & \text{if } i = M \text{ or } j = 0 \\ (-1)^M (i-j+1) \alpha_{i(j-1)}^{(M-1)}, & \text{otherwise,} \end{cases} \quad \alpha_{3,ij}^{(M)} = \begin{cases} 0, & \text{if } i = 1 \text{ or } j = 0 \\ \frac{(-1)^{M-1}}{2} \alpha_{(i-1)(j-1)}^{M-1}, & \text{otherwise,} \end{cases}$$

and $\alpha_{10}^{(1)} = 0$, $\alpha_{11}^{(1)} = \frac{1}{2\pi}$. Additionally, $I_{m+1}[\tilde{u}^{(m+1)}, j, k] = O\left(\frac{1}{k}\right)$, and if $u \in C^{m+2}(\Omega)$ then (25) holds for $1 \leq M \leq m+2$.

Proof. We prove this lemma using induction on M . When $M = 1$, the lemma is true since $c_k = \frac{1}{2\pi} \frac{h}{k} I_1[\tilde{u}^{(1)}, 1, k]$ as obtained from integration by parts. By induction hypothesis, assume that the result is true for any natural number $M \leq m$. Using Lemma 3.2, the coefficient c_k can be expressed as

$$c_k = \sum_{i=1}^M \sum_{j=0}^i \frac{h^i}{k^M} \alpha_{ij}^{(M)} \left[\frac{(-1)^{M+1} j}{k} I_{M+1}[\tilde{u}^{(i)}, j-1, k] + \frac{(-1)^M (i-j)}{k} I_{M+1}[\tilde{u}^{(i)}, j+1, k] \right. \\ \left. + \frac{(-1)^N h}{2} \frac{1}{k} I_{M+1}[\tilde{u}^{(i+1)}, j+1, k] \right]. \quad (26)$$

After re-indexing, c_k becomes

$$c_k = \sum_{i=1}^{M+1} \sum_{j=0}^i \frac{h^i}{k^{M+1}} \alpha_{ij}^{(M+1)} I_{M+1}[\tilde{u}^{(i)}, j, k].$$

Thus, equation (25) is true for $1 \leq M \leq m+1$. This completes the proof by induction for $u \in X^m$. Additionally, since $\tilde{u}(\cos(\cdot)) \in C_{\text{pw}}^{m+2}[-\pi, \pi]$, there exist discontinuities of $(m+1)$ -th derivative of $\tilde{u}(\cos \theta)$ at $\{s_\ell\}_{\ell=0}^{n_d}$ for some $n_d \in \mathbb{N}$ such that $[-\pi, \pi] = \cup_{\ell=1}^{n_d} [s_{\ell-1}, s_\ell]$. Therefore,

$$I_{m+1}[\tilde{u}^{(m+1)}, j, k] = \frac{(-1)^{m+1}}{k} \sum_{\ell=1}^{n_d} \left[\left(\tilde{u}^{(m+1)}(\cos \theta) \sin^j(\theta) \cos^{i-j}(\theta) \zeta_{m+2}(k\theta) \right)_{s_{\ell-1}}^{s_\ell} \right. \\ \left. - \int_{s_{\ell-1}}^{s_\ell} \left(\tilde{u}^{(m+1)}(\cos \theta) \sin^j(\theta) \cos^{i-j}(\theta) \right)' \zeta_{m+2}(k\theta) d\theta \right] = O\left(\frac{1}{k}\right).$$

This completes the proof for case $u \in X^{m+2}(\Omega)$. If $u \in C^{m+2}(\Omega)$ then another application of recursive relation Lemma 3.2 proves (25) for $M = m + 2$. \square

While estimating the decay rate of c_k in terms of k and h , using Lemma 3.3 we have achieved the optimal decay in terms of k and now, we would like to estimate the optimal bound in terms of h . To do so, we re-write the integral (19) as a function of μ below and investigate it's behavior as $\mu \rightarrow 0$.

$$I_M[\tilde{u}^{(i)}, j, k](\mu) = \int_{-\pi}^{\pi} \tilde{u}^{(i)}\left(\frac{\mu}{h} \cos \theta\right) \sin^j(\theta) \cos^{i-j}(\theta) \zeta_M(k\theta) d\theta, \quad (27)$$

where $\mu \in [-h, h]$. Observe that $I_M[\tilde{u}^{(i)}, j, k](h) = I_M[\tilde{u}^{(i)}, j, k]$. In the following lemma we estimate the bound for (27).

Lemma 3.4. *For integers $0 \leq j \leq i \leq m$ with $i < k$ and $0 \leq M$ the following estimates hold:*

i. *If $u \in X^m(\Omega)$ then*

$$I_M[\tilde{u}^{(i)}, j, k](\mu) = O\left(\mu^{\min\{k, m+1\}-i}\right). \quad (28)$$

ii. *If $u \in C^{m+2}(\Omega)$ then*

$$I_M[\tilde{u}^{(i)}, j, k](\mu) = O\left(\mu^{\min\{k, m+2\}-i}\right), \quad (29)$$

where $\mu \in [-h, h] \subseteq [-1, 1]$.

Proof. (i). We first investigate the regularity of the integral $I_M[\tilde{u}^{(i)}, j, k](\mu)$ defined in (27) at $\mu = 0$. If $u \in X^m(\Omega)$, using Leibniz rule we deduce that $I_M[\tilde{u}^{(i)}, j, k](\mu)$ is $m - i$ times differentiable. In particular the derivatives of $I_M[\tilde{u}^{(i)}, j, k](\mu)$ are given by

$$\frac{d^n}{d\mu^n} I_M[\tilde{u}^{(i)}, j, k](\mu) = \frac{1}{2^n} \int_{-\pi}^{\pi} \tilde{u}^{(i+n)}\left(\frac{\mu}{h} \cos \theta\right) \sin^j(\theta) \cos^{i-j+n}(\theta) \zeta_M(k\theta) d\theta = \frac{1}{2^n} I_M[\tilde{u}^{(i+n)}, j, k](h), \quad (30)$$

for $0 \leq n \leq m - i$. Since u is piecewise C^{m+2} which implies that $(m + 1 - i)^{th}$ derivative of $I_M[\tilde{u}^{(i)}, j, k](h)$ exists. Now doing a finite Taylor expansion of $I_M[\tilde{u}, j, k](\mu)$ at $\mu = 0$, we have

$$I_M[\tilde{u}^{(i)}, j, k](\mu) = \sum_{n=0}^{m-i} I_M[\tilde{u}^{(i+n)}, j, k](0) \frac{\mu^n}{2^n n!} + O\left(\mu^{m+1-i}\right). \quad (31)$$

We now estimate the right hand side of equation (31). For $0 \leq n \leq m - i$,

$$I_M[\tilde{u}^{(i+n)}, j, k](0) = \tilde{u}^{(i+n)}(0) \int_{-\pi}^{\pi} \sin^j(\theta) \cos^{i+n-j}(\theta) \zeta_M(k\theta) d\theta = 0, \quad (32)$$

if $0 \leq j \leq i + n < k$ or $n < k - i$. Indeed, equation (32) follows by expanding powers of sine and cosine in terms of the complex exponential and using $\int_{-\pi}^{\pi} \cos(k\theta) d\theta = \int_{-\pi}^{\pi} \sin(k\theta) d\theta = 0$ for all non-zero k . Therefore, if $k \leq m$, the first non-zero term of the summation in equation (31) occur at $n = k - i$ and we obtain $I_M[\tilde{u}^i, j, k](\mu) = O(\mu^{k-i})$. If $k > m$, then every term in the summation of (31) becomes zero because of (32), which implies $I_M[\tilde{u}^i, j, k](\mu) = O(\mu^{m+1-i})$. Combining these two cases we get the desired result when $u \in X^m(\Omega)$. For part (ii), using Leibniz rule we deduce that $I_M[\tilde{u}^{(i)}, j, k](\mu)$ is $m + 2 - i$ times differentiable. Now doing a finite Taylor expansion of $I_M[\tilde{u}^{(i)}, j, k](\mu)$ at $\mu = 0$, we have

$$I_M[\tilde{u}^{(i)}, j, k](\mu) = \sum_{n=0}^{m+1-i} I_M[\tilde{u}^{(i+n)}, j, k](0) \frac{\mu^n}{2^n n!} + O\left(\mu^{m+2-i}\right).$$

Now, following the similar arguments which we carried out for $u \in X^m(\Omega)$, we get the desired bound that $I_M[\tilde{u}^{(i)}, j, k](\mu) = O(\mu^{k-i}) + O(\mu^{m+2-i})$ if $u \in C^{m+2}(\Omega)$. \square

Theorem 3.5. Let $k \geq 1$ be an integer and let c_k denote the k -th Chebyshev coefficient of \tilde{u} defined as in (17). Then the following holds:

i. If $u \in X^m(\Omega)$ then

$$|c_k| \leq C \frac{h^{\min\{k, m+1\}}}{k^{m+2}}. \quad (33)$$

ii. If $u \in C^{m+2}(\Omega)$ then

$$|c_k| \leq C \frac{h^{\min\{k, m+2\}}}{k^{m+2}}, \quad (34)$$

where $h = b - a$ is the length of Ω such that $h \leq 1$ and C is a positive constant independent of k and h .

Proof. (i). If $u \in X^m(\Omega)$, using Lemma 3.3 for $M = m + 1$, an expression for c_k can be obtained as

$$c_k = \sum_{i=1}^m \sum_{j=0}^i \alpha_{ij}^{(m+1)} \frac{h^i}{k^{m+1}} I_{m+1}[\tilde{u}^{(i)}, j, k] + \sum_{j=0}^{m+1} \alpha_{(m+1)j}^{(m+1)} \frac{h^{m+1}}{k^{m+1}} I_{m+1}[\tilde{u}^{(m+1)}, j, k]. \quad (35)$$

Additionally, in Lemma 3.3 we have shown that $I_{m+1}[\tilde{u}^{(m+1)}, j, k] = O(1/k)$. Using this bound, the second term in (35) can be estimated as

$$\left| \sum_{j=0}^{m+1} \alpha_{(m+1)j}^{(m+1)} \frac{h^{m+1}}{k^{m+1}} I_{m+1}[\tilde{u}^{(m+1)}, j, k] \right| \leq C \frac{h^{m+1}}{k^{m+2}}.$$

Using the recurrence relation for $I_{m+1}[\tilde{u}^{(i)}, j, k]$ described in Lemma 3.2, the first sum in equation (35) can be expressed as

$$c_k = \sum_{i=1}^m \frac{h^i}{k^{m+2}} \sum_{j=0}^i \alpha_{ij}^{(m+1)} \left[(-1)^m j I_{m+2}[\tilde{u}^{(i)}, j-1, k] - (-1)^m (i-j) I_{m+2}[\tilde{u}^{(i)}, j+1, k] - \frac{(-1)^m}{2} h I_{m+2}[\tilde{u}^{(i+1)}, j+1, k] \right].$$

Thus, using Lemma 3.4 and observing the fact $I_M[\tilde{u}^{(i)}, j, k](h) = I_M[\tilde{u}^{(i)}, j, k]$, we obtain

$$\begin{aligned} \left| I_{m+2}[\tilde{u}^{(i)}, j \pm 1, k] \right| &\leq C h^{\min\{k, m+1\}-i}, \\ \left| I_{m+2}[\tilde{u}^{(i+1)}, j+1, k] \right| &\leq C h^{\min\{k, m+1\}-(i+1)}. \end{aligned}$$

Since the constants in the above summations are dependent only on i , j and m , and independent of h and k we obtain the required result. For part (ii), if $u \in C^{m+2}(\Omega)$, using Lemma 3.3 for $M = m + 2$, an expression for c_k can be obtained as

$$c_k = \sum_{i=1}^{m+2} \sum_{j=0}^i \frac{h^i}{k^{m+2}} \alpha_{ij}^{(m+2)} I_{m+2}[\tilde{u}^{(i)}, j, k], \quad (36)$$

using Lemma 3.4 and the fact $I_{m+2}[\tilde{u}^{(i)}, j, k] = I_{m+2}[\tilde{u}^{(i)}, j, k](h)$, we get

$$\left| I_{m+2}[\tilde{u}^{(i)}, j, k] \right| \leq C h^{\min\{k, m+2\}-i}. \quad (37)$$

Since α_{ij}^{m+2} in equation (36) depends only on i , j and m , and independent of h and k , we obtain the required bound for c_k when $u \in C^{m+2}(\Omega)$. \square

In view of the singular integration scheme, note that it is important to investigate the convergence of the discrete Chebyshev expansion of a function $u \in X^m(\Omega)$ and the error in $|c_k - \tilde{c}_k|$ which is the approximation of the continuous coefficients c_k by their discrete counterparts \tilde{c}_k . The following result briefly describes the error in the approximation $|c_k - \tilde{c}_k|$.

Theorem 3.6. *Let $0 \leq k \leq n-1$ be an integer and u_l as defined in (17). Let c_k denote the k -th Chebyshev coefficient of \tilde{u} and \tilde{c}_k its discrete counterpart, then the following hold:*

i. *If $u \in X^m(\Omega)$ then*

$$|c_k - \tilde{c}_k| \leq C \frac{h^{\min\{n+1, m+1\}}}{n^{m+2}}. \quad (38)$$

ii. *If $u \in C^{m+2}(\Omega)$ then*

$$|c_k - \tilde{c}_k| \leq C \frac{h^{\min\{n+1, m+2\}}}{n^{m+2}}, \quad (39)$$

where $h \leq 1$ is the length of Ω , n is the number of terms in discrete Chebyshev expansion of \tilde{u} , that is, $\tilde{u}(t) \approx \sum_{k=0}^{n-1} \tilde{c}_k T_k(t)$, and C is some constant independent of h and n .

Proof. The Chebyshev series expansion of u_l is given by

$$\tilde{u}(t) = \sum_{k=0}^{\infty} c_k T_k(t) = \sum_{k=0}^{n-1} c_k T_k(t) + R_n(t), \text{ where } R_n(t) = \sum_{k=n}^{\infty} c_k T_k(t). \quad (40)$$

From equation (40) it is clear that $(\tilde{u} - R_n)(t)$ is a polynomial with degree at most $n-1$ implying that its discrete and continuous Chebyshev coefficients are equal [15, Theorem 6.7]. We obtain

$$(\tilde{u} - R_n)(t) = \sum_{k=0}^{n-1} c_k T_k(t), \text{ and } c_k = \frac{\gamma_k}{n} \sum_{i=0}^{n-1} (\tilde{u} - R_n)(t_i) T_k(t_i), \quad \gamma_k = \begin{cases} 1, & \text{if } k=0 \\ 2, & \text{otherwise,} \end{cases} \quad (41)$$

where $t_i = \cos(\pi \frac{2i+1}{2n})$, $0 \leq i < n$. The error in the continuous and the discrete Chebyshev coefficients becomes

$$\tilde{c}_k - c_k = \frac{\gamma_k}{n} \sum_{i=0}^{n-1} R_n(t_i) T_k(t_i) = \frac{\gamma_k}{n} \sum_{j=n}^{\infty} c_j \left[\sum_{i=0}^{n-1} T_j(t_i) T_k(t_i) \right]. \quad (42)$$

Using [15, Section 4.6], one can derive the following version of the discrete orthogonality rule: For integers $0 \leq k \leq n-1$ and $1 \leq n \leq j$ is given by

$$\sum_{i=0}^{n-1} T_j(y_i) T_k(y_i) = \frac{1}{2} \begin{cases} (-1)^l n, & \text{if } j+k=2nl, \quad l \in \mathbb{N} \\ (-1)^l n, & \text{if } j-k=2nl, \quad l \in \mathbb{N} \\ 0, & \text{otherwise,} \end{cases} \quad (43)$$

where $y_i = \cos(\pi \frac{2i+1}{2n})$, $0 \leq i < n$. Using the identity (43), we obtain

$$\tilde{c}_k - c_k = \frac{\gamma_k}{2} \left[\sum_{i=1}^{\infty} (-1)^i c_{2ni-k} + \sum_{i=1}^{\infty} (-1)^i c_{2ni+k} \right]. \quad (44)$$

For every $0 \leq k < n$, using Theorem 3.5, we deduce

$$|c_k - \tilde{c}_k| \leq c \sum_{i=1}^{\infty} \left[\frac{h^{\min\{2ni-k, m+1\}}}{(2ni-k)^{m+2}} + \frac{h^{\min\{2ni+k, m+1\}}}{(2ni+k)^{m+2}} \right].$$

To capture the appropriate power of h , we split the summation in what follows. There exist integer $N_0 \geq 1$ such that $2n(N_0 - 1) + n - 1 \leq m + 1 < 2nN_0$. For this choice of N_0 , observe that the exponent on h has the following three cases.

- i. If $1 \leq i \leq N_0 - 1$ then $2ni - k < 2ni + k \leq m + 1$ for each $0 \leq k \leq n - 1$.
- ii. If $i = N_0$ then $n + 1 \leq 2nN_0 - k$ and $m + 1 < 2nN_0 + k$ for each $0 \leq k \leq n - 1$.
- iii. If $i \geq N_0 + 1$ then $m + 1 \leq 2ni - k < 2ni + k$ for each $0 \leq k \leq n - 1$.

Therefore, we get

$$|c_k - \tilde{c}_k| \leq c \frac{h^{n+1}}{n^{m+2}} \left(\sum_{i=1}^{N_0-1} \left[\frac{h^{n(2i-1)-k-1}}{(2i - \frac{k}{n})^{m+2}} + \frac{h^{n(2i-1)+k-1}}{(2i + \frac{k}{n})^{m+2}} \right] \right) + \frac{h^{\min\{2nN_0-k, m+1\}}}{(2N_0 - \frac{k}{n})^{m+2}} \\ + c \frac{h^{m+1}}{n^{m+2}} \left(\frac{1}{(2N_0 + \frac{k}{n})^{m+2}} + \sum_{i=N_0+1}^{\infty} \left[\frac{1}{(2i - \frac{k}{n})^{m+2}} + \frac{1}{(2i + \frac{k}{n})^{m+2}} \right] \right).$$

For $0 \leq k \leq n - 1$, the terms $\frac{1}{(2i - \frac{k}{n})^{m+2}}$ and $\frac{1}{(2i + \frac{k}{n})^{m+2}}$ are bounded by $\frac{1}{(2i-1)^{m+2}}$ and $\frac{1}{(2i)^{m+2}}$ respectively. Thus, the infinite series is finite and the result follows. The proof when $u \in C^{m+2}$ can be carried out in a similar manner. \square

Remark 3.7. Let n be a positive integer and \tilde{c}_k denote the k -th discrete Chebyshev coefficient of \tilde{u} defined as (17) for $0 \leq k < n$. Using triangle inequalities in Theorem 3.6 and Theorem 3.5, the following holds:

- i. If $u \in X^m(\Omega)$ then

$$|\tilde{c}_k| \leq C \frac{h^{\min\{k, m+1\}}}{k^{m+2}}. \quad (45)$$

- ii. If $u \in C^{m+2}(\Omega)$ then

$$|\tilde{c}_k| \leq C \frac{h^{\min\{k, m+2\}}}{k^{m+2}}, \quad (46)$$

where $h = b - a$ is the length of Ω and C is some constant independent of h and k .

Since $T_k(t)$ is a polynomial, the approximation $\sum_{k=0}^{n-1} \tilde{c}_k T_k(t)$ is a polynomial approximation to \tilde{u} . More precisely, denoting $L^n[\tilde{u}](t) = \sum_{k=0}^{n-1} \tilde{c}_k T_k(t)$, it is easy to see that $L^n[\tilde{u}]$ is the n -th order Lagrange interpolating polynomial corresponding to the roots of the Chebyshev polynomial $T_n(t)$. Interestingly, using [7, Section 2.5.5], one can notice that the FF-Rule is an interpolatory quadrature and

$$\mathcal{K}_{ff}^n[\tilde{u}] = \frac{h}{2} \int_{-1}^1 L^n[\tilde{u}](t) dt. \quad (47)$$

In the following theorem we describe a convergence result for the FF-Rule approximation of the integral of \tilde{u} , which follows from the results described above.

Theorem 3.8. *Let n be a positive integer and $\mathcal{K}_{ff}^n[\tilde{u}]$ be the FF-Rule approximation of the integral of u on interval Ω with n discretization points where \tilde{u} is defined as in (17). Then the following holds:*

- i. If $u \in X^m(\Omega)$ then

$$\left| \int_a^b u(y) dy - \mathcal{K}_{ff}^n[\tilde{u}] \right| \leq C \frac{h^{\min\{n+1+n_0, m+2\}}}{n^{m+2}}.$$

- ii. If $u \in C^{m+2}(\Omega)$ then

$$\left| \int_a^b u(y) dy - \mathcal{K}_{ff}^n[\tilde{u}] \right| \leq C \frac{h^{\min\{n+1+n_0, m+3\}}}{n^{m+2}},$$

where $n_0 = 1$ if n is odd and $n_0 = 0$ otherwise, $h \leq 1$ and C is a constant independent of h and n .

Proof. Using equation (47) and the identity related to the integral of a Chebyshev polynomial given in [7, Section 2.5.5], one can notice that the error in the FF-Rule approximation can be written as follows:

$$\begin{aligned} \left| \int_a^b u(y) dy - \mathcal{K}_{ff}^n[\tilde{u}] \right| &= \left| \frac{h}{2} \int_{-1}^1 \tilde{u}(t) dt - \frac{h}{2} \int_{-1}^1 L^n[\tilde{u}](t) dt \right| \\ &= \frac{h}{2} \left| \int_{-1}^1 \sum_{k=0}^{\infty} c_k T_k(t) dt - \int_{-1}^1 \sum_{k=0}^{n-1} \tilde{c}_k T_k(t) dt \right| \\ &\leq \frac{h}{2} \sum_{k=n+n_0}^{\infty} |c_k| \left| \int_{-1}^1 T_k(t) dt \right| + \frac{h}{2} \sum_{k=0}^{n-1+n_0} |c_k - \tilde{c}_k| \left| \int_{-1}^1 T_k(t) dt \right|. \end{aligned} \quad (48)$$

Now using Theorem 3.6 for $u \in X^m$ and $u \in C^{m+2}$ in equation (48) we can prove (i) and (ii) respectively. \square

The decay rate of discrete Chebyshev coefficients presented in Remark 3.7 and the FF-rule approximation derived in Theorem 3.8 are demonstrated numerically the following examples.

Example 3.9. Consider the function $u(x) = x^3|x| + x^3 + x^2 + x + 1$ in the interval $[-\frac{1}{2N}, \frac{1}{N}]$ where $N = 2, 4, 8, \dots, 256$. That is, the length of the interval $h = \frac{3}{2N}$. Table (1) demonstrates the decay rates of the discrete Chebyshev coefficients \tilde{c}_k of $\tilde{u}(x) = u(\xi(x))$, where $1 \leq k \leq 10$, $\xi(t) = ht/2 + 1/4N$. Since $u \in X^m[-1, 1]$, with $m = 3$, according to Remark 3.7, \tilde{c}_k converge to zero with the rate $\min\{k, 4\}$ as $h \rightarrow 0$, for every $k \geq 1$, which is what the columns in the table (1) show. Hence, the numerical convergence rates exactly align with the theoretically estimated convergence rates.

N	\tilde{c}_1	\tilde{c}_2	\tilde{c}_3	\tilde{c}_4	\tilde{c}_5	\tilde{c}_6	\tilde{c}_7	\tilde{c}_8	\tilde{c}_9	\tilde{c}_{10}
4	1.33	2.35	3.30	4.00	4.00	4.00	4.00	4.00	4.00	4.00
8	1.13	2.16	3.18	4.00	4.00	4.00	4.00	4.00	4.00	4.00
16	1.05	2.08	3.10	4.00	4.00	4.00	4.00	4.00	4.00	4.00
32	1.02	2.04	3.05	4.00	4.00	4.00	4.00	4.00	4.00	4.00
64	1.01	2.02	3.03	4.00	4.00	4.00	4.00	4.00	4.00	4.00
128	1.01	2.01	3.01	4.00	4.00	4.00	4.00	4.00	4.00	4.00
256	1.00	2.00	3.01	4.00	4.00	4.00	4.00	4.00	4.01	4.00

Table 1: Order of convergence of Chebyshev coefficients \tilde{c}_k of $\tilde{u} \in X^m[-1, 1]$ with $m = 3$. The expected decay rate of \tilde{c}_k is $\min\{k, m + 1\} = \min\{k, 4\}$. The theoretical decay rate match with their numerical counterparts.

4 Quadrature Analysis

In this section, we present error analysis for single patch and later generalize this idea for arbitrary number of patches. We consider the integration patch $\Omega = [a, b]$ and length $h = b - a$. For analysis in single patch we avoid mentioning patch number ℓ . Recall from Section 2, for the target point $x \in \Omega$,

$$\mathcal{K}[u](x) = \int_{-1}^1 g_\alpha(|x - \xi(t)|) u(\xi(t)) dt, \quad \beta_k(x) = \frac{h}{2} \int_{-1}^1 g_\alpha(|x - \xi(t)|) T_k(t) dt, \quad (49)$$

where $\xi(t) = \frac{h}{2}t + \frac{a+b}{2}$ and the kernel is defined as in (2). The error in singular quadrature is given by

$$E_{\text{sing}}^n[u](x) = |\mathcal{K}[u](x) - \mathcal{K}_{\text{sing}}^n[u](x)| \leq E_1^n[u](x) + E_2^n[u](x) + E_3^n[u](x), \quad (50)$$

where $\mathcal{K}_{\text{sing}}^n[u]$ is defined as in equation (16), and $E_1^n[u], E_2^n[u], E_3^n[u]$ are given by

$$E_1^n[u](x) = \left| \mathcal{K}[u](x) - \sum_{k=0}^{n-1} c_k \beta_k(x) \right|, \quad (51)$$

$$E_2^n[u](x) = \sum_{k=0}^{n-1} |c_k - \tilde{c}_k| |\beta_k(x)|, \quad (52)$$

$$E_3^n[u](x) = \sum_{k=0}^{n-1} |\tilde{c}_k| |\beta_k - \tilde{\beta}_k(x)|. \quad (53)$$

Recall from Section 2, $\tilde{\beta}_k$ is defined as in equation (16), and c_k, \tilde{c}_k are the k -th continuous and discrete Chebyshev coefficient of the density u respectively. Term E_1^n denotes error in truncation of Chebyshev expansion, E_2^n is the error in the approximation of continuous Chebyshev coefficients c_k by discrete coefficients \tilde{c}_k , and E_3^n represents error the approximation of the weights $\beta_k(x)$ by the singular integration strategy discussed in Section 2. In the following we establish an error estimate for all the three error terms separately.

4.1 Error in truncation

We now compute the bound for the first error term $E_1^n[u]$, for that we need the decay rate of c_k on Ω , which we derived in Theorem 3.5, and in what follows, we find a bound for the continuous wights $\beta_k(x)$, which holds uniformly for each $x \in \Omega$.

Lemma 4.1. *For $x \in \Omega$,*

$$|\beta_k(x)| \leq C \begin{cases} \frac{h |\log h|}{k^2} + \frac{h \log k}{k}, & \text{if } \alpha = 0, k > 1 \\ \frac{h^{1-\alpha}}{k^{1-\alpha}}, & \text{if } 0 < \alpha < 1, k \geq 1. \end{cases} \quad (54)$$

Proof. For $x \in \Omega$, there exists $t_x \in [-1, 1]$ such that $\xi(t_x) = x$. Therefore, β_k can be written as

$$\beta_k(x) = \frac{h}{2} \int_{-1}^1 g_\alpha(|\xi(t_x) - \xi(t)|) T_k(t) dt = \begin{cases} \frac{h}{2} \int_{-1}^1 \log \left(\left| \frac{h}{2} (t_x - t) \right| \right) T_k(t) dt, & \text{if } \alpha = 0 \\ \left(\frac{h}{2} \right)^{1-\alpha} \int_{-1}^1 |t_x - t|^{-\alpha} T_k(t) dt, & \text{if } 0 < \alpha < 1. \end{cases} \quad (55)$$

For $\alpha = 0$, the integral can split as

$$\beta_k(x) = \frac{h}{2} \log \left(\frac{h}{2} \right) \int_{-1}^1 T_k(t) dt + \frac{h}{2} \int_{-1}^1 \log |t_x - t| T_k(t) dt. \quad (56)$$

The integral of k -th Chebyshev polynomial is $\int_{-1}^1 T_k(t) dt = O(1/k^2)$ [18]. Now utilizing [8, Lemma 3.1] for case $0 < \alpha < 1$ in equation (55) and log kernel in (56), we obtain the required result. \square

Now, we present the theorem which gives a bound for E_1^n in equation (51).

Theorem 4.2. *If $u \in X^m(\Omega)$ then*

$$E_1^n[u](x) \leq C \begin{cases} \frac{h^{\min\{n+1, m+2\}} |\log h|}{n^{m+3}} + \frac{h^{\min\{n+1, m+2\}} \log n}{n^{m+2}}, & \text{if } \alpha = 0 \\ \frac{h^{\min\{n+1-\alpha, m+2-\alpha\}}}{n^{m+2-\alpha}}, & \text{if } 0 < \alpha < 1. \end{cases}$$

where h is length of Ω , n is number of terms in Chebyshev expansion of u and C is some constant independent of h and n .

Proof. The Chebyshev series of u converges absolutely and uniformly. Therefore, employing the Chebyshev series expansion of $u(y)$, we have

$$E_1^n[u](x) = \left| \mathcal{K}[u](x) - \sum_{k=0}^{n-1} c_k \beta_k(x) \right| = \left| \int_{-1}^1 g_\alpha(|x - \xi(t)|) \left[\sum_{k=n}^{\infty} c_k T_k(t) \right] dt \right| \leq \sum_{k=n}^{\infty} |c_k| |\beta_k(x)|. \quad (57)$$

Employing Theorem 3.5 and Lemma 4.1, we have

$$E_1^n[u](x) \leq Ch^{\min\{n+1, m+2\}} \left[\sum_{k=n}^{\infty} \frac{\log k}{k^{m+3}} + \log(h) \sum_{k=n}^{\infty} \frac{1}{k^{m+4}} \right] \leq Ch^{\min\{n+1-\alpha, m+2-\alpha\}} \sum_{k=n}^{\infty} \frac{1}{k^{m+3-\alpha}},$$

for $\alpha = 0$ and $0 < \alpha < 1$ respectively. Hence, from Euler's summation formula [1, Theorem 3.1], the theorem follows. \square

We proceed to estimate the error term E_2^n in (52), which represents the approximation of continuous Chebyshev coefficients by their discrete counterparts.

Theorem 4.3. *If $u \in X^m(\Omega)$ then*

$$E_2^n[u](x) \leq C \begin{cases} \frac{h^{\min\{n+2, m+2\}} (\log n)^2}{n^{m+2}} + \frac{h^{\min\{n+2, m+2\}} |\log h|}{n^{m+3}}, & \text{if } \alpha = 0 \\ \frac{h^{\min\{n+2-\alpha, m+2-\alpha\}}}{n^{m+2-\alpha}}, & \text{if } 0 < \alpha < 1, \end{cases}$$

where h is length of Ω , n is number of terms in Chebyshev expansion of u and C is some constant independent of h and n .

Proof. For $0 < \alpha < 1$, it is easy to see that $|\beta_0(x)| \leq Ch^{1-\alpha}$ and $\sum_{k=1}^{n-1} \frac{1}{k^{1-\alpha}} = O(n^\alpha)$ using Euler summation formula [1, Theorem 3.1]. Utilizing Lemma (4.1) for estimating $|\beta_k(x)|$, we obtain

$$\sum_{k=0}^{n-1} |\beta_k(x)| \leq |\beta_0(x)| + C \sum_{k=1}^{n-1} \frac{h^{1-\alpha}}{k^{1-\alpha}} = O(h^{1-\alpha} n^\alpha). \quad (58)$$

Similarly, for $\alpha = 0$, $|\beta_0(x)| \leq Ch |\log h|$, $|\beta_1(x)| \leq Ch |\log h|$ and $\sum_{k=1}^{n-1} \frac{\log k}{k} = O((\log n)^2)$ using Euler summation formula [1, Theorem 3.1]. We obtain

$$\sum_{k=0}^{n-1} |\beta_k(x)| \leq |\beta_0(x)| + |\beta_1(x)| + Ch \sum_{k=2}^{n-1} \frac{\log k}{k} + Ch |\log h| \sum_{k=2}^{n-1} \frac{1}{k^2} \leq C \left[h (\log n)^2 + \frac{h |\log h|}{n} \right]. \quad (59)$$

By applying Theorem 3.6, the error term E_2^n can be deduced to

$$E_2^n[u](x) = \sum_{k=0}^{n-1} |c_k - \tilde{c}_k| |\beta_k(x)| \leq C \frac{h^{\min\{n+1, m+1\}}}{n^{m+2}} \sum_{k=0}^{n-1} |\beta_k(x)|.$$

Thus, the proof follows from equations (58) and (59), respectively. \square

4.2 Error in the approximation of weights

Before finding a bound on error term E_3^n (53), let us recall the change of variable which we incorporated in singular integral, that is, for $p \geq 2$

$$\psi_p(t) = \frac{2[v_p(t)]^p}{[v_p(t)]^p + [v_p(-t)]^p}, \quad v_p(t) = \left(\frac{1}{2} - \frac{1}{p}\right)t^3 + \frac{t}{p} + \frac{1}{2}, \quad -1 \leq t \leq 1.$$

Now, we state properties of the change of variables ψ_p and v_p in the following lemma.

Lemma 4.4. *For an integer $p \geq 2$, the following holds:*

1. *The function v_p is strictly increasing and $v_p(t) = (t+1) \cdot q_p(t)$, where $q_p(t) = \left(\frac{1}{2} - \frac{1}{p}\right)(t^2 - t) + \frac{1}{2}$.*
2. *For $t \in [-1, 1]$, $q_p(t) > 0$ and $\psi_p(t) = (t+1)^p \cdot Q_p(t)$, where $Q_p(t) = \frac{2[q_p(t)]^p}{[v_p(t)]^p + [v_p(-t)]^p}$.*
3. *The derivative of ψ_p is $\psi_p'(t) = (t+1)^{p-1} \cdot R_p(t)$, where $R_p(t) = (t+1) \cdot Q_p'(t) + p \cdot Q_p(t)$.*
4. *The function ψ_p has a zero at $t = -1$ of order strictly p .*
5. *The functions Q_p , $1/Q_p$ and R_p are infinitely differentiable on $[-1, 1]$.*

Proof. Assertions (1), (2) and (3) follow from the definition of v_p and ψ_p . Clearly $v_p(-1) = 0$, $\psi_p(-1) = 0$. Using the Leibniz rule of derivative, we have

$$\psi_p^{(j)}(t) = \sum_{i=0}^{j-1} \binom{j}{i} \left[\frac{d^i}{dt^i} (t+1)^p \right] Q_p^{(j-i)}(t) + \frac{p!}{(p-j)!} (t+1)^{p-j} Q_p(t).$$

Therefore, for $1 \leq j \leq p-1$, $\psi_p^{(j)}(-1) = 0$. Since $Q_p(t) \neq 0$ for every $t \in [-1, 1]$, $\psi_p^{(p)}(-1) \neq 0$. Hence (4) is proved. Since the numerator and denominator of Q_p are the non-zero polynomials in t , Q_p and $1/Q_p$ are infinitely differentiable. Moreover, it is clear that the smoothness of Q_p implies the smoothness of R_p . Thus, the assertion (5) is proved. \square

To find a bound on E_3^n (53) which is,

$$E_3^n[u](x) = \left| \sum_{k=0}^{n-1} \tilde{c}_k \left(\beta_k(x) - \tilde{\beta}_k(x) \right) \right| \leq \sum_{k=0}^{n-1} |\tilde{c}_k| \left| \beta_k(x) - \tilde{\beta}_k(x) \right|,$$

it is important to compute bounds for $|\beta_k(x) - \tilde{\beta}_k(x)|$ uniformly in x and k . Therefore, consider

$$|\beta_k(x) - \tilde{\beta}_k(x)| \leq |\beta_{k,L}(x) - \tilde{\beta}_{k,L}(x)| + |\beta_{k,R}(x) - \tilde{\beta}_{k,R}(x)|, \quad (60)$$

where $\beta_{k,L}$, $\beta_{k,R}$, $\tilde{\beta}_{k,L}$ and $\tilde{\beta}_{k,R}$ are as defined in (15) and (16) respectively for the single patch Ω . Now, we find the estimates for $|\beta_k(x) - \tilde{\beta}_k(x)|$ by combining the errors for both terms on the right hand-side of (60) for the cases $\alpha = 0$ and $0 < \alpha < 1$ separately. We start with $|\beta_{k,L}(x) - \tilde{\beta}_{k,L}(x)|$. For every $x \in \Omega$, define $\xi(t_x) = x$, where $\xi : [-1, 1] \rightarrow \Omega$ is defined by $\xi(t) = \frac{h}{2}t + \frac{a+b}{2}$. The expression for $\beta_{k,L}$ and $\beta_{k,R}$ for $x \in \Omega \setminus \{a, b\}$ can be simplified as

$$\beta_{k,L}(x) = \frac{h}{2} \int_{-1}^1 g_\alpha \left(\frac{h}{2}(t_x + 1)\psi_p \left(-\frac{1+\tau}{2} \right) \right) T_k(\psi_{p,L}(t_x, \tau)) \psi_{p,L}'(t_x, \tau) d\tau, \quad (61)$$

$$\beta_{k,R}(x) = \frac{h}{2} \int_{-1}^1 g_\alpha \left(\frac{h}{2}(1 - t_x)\psi_p \left(-\frac{1-\tau}{2} \right) \right) T_k(\psi_{p,R}(t_x, \tau)) \psi_{p,R}'(t_x, \tau) d\tau, \quad (62)$$

where

$$\psi_{p,L}(t_x, \tau) = t_x - (t_x + 1)\psi_p\left(-\frac{1+\tau}{2}\right), \quad \psi_{p,R}(t_x, \tau) = t_x + (1 - t_x)\psi_p\left(-\frac{1-\tau}{2}\right), \quad (63)$$

$$\psi'_{p,L}(t_x, \tau) = \frac{t_x + 1}{2}\psi'_p\left(-\frac{1+\tau}{2}\right), \quad \psi'_{p,R}(t_x, \tau) = \frac{1 - t_x}{2}\psi'_p\left(-\frac{1-\tau}{2}\right), \quad (64)$$

for $\tau \in [-1, 1]$, $p \geq 2$. Note that the derivative $\psi'_{p,L}, \psi'_{p,R}$ are with respect to variable τ . If $x = a$, observe that only integral $\beta_{k,L}$ remains and for $x = b$, only $\beta_{k,R}$ remains. The calculations can be divided in cases $\alpha = 0$ and $0 < \alpha < 1$, which we write in the following two lemmas.

Lemma 4.5. *Let $x \in \Omega$ and $g_\alpha(|x - y|) = \log|x - y|$, that is $\alpha = 0$. Then, for $k \geq 0$*

$$\left| \beta_k(x) - \tilde{\beta}_k(x) \right| \leq C \frac{h \log n_\beta}{n_\beta^{2p}}, \quad (65)$$

where $p \geq 2$ is an integer, h is length of patch Ω , n_β denotes the number of quadrature nodes in the FF-Rule approximation both $\tilde{\beta}_{k,L}(x)$ and $\beta_{k,R}(x)$, and C is some constant independent of h and n_β .

Proof. We first estimate the error $|\beta_{k,L}(x) - \tilde{\beta}_{k,L}(x)|$ for $x \in \Omega \setminus \{a\}$. Utilizing (2) of Lemma 4.4, decompose the integrand in (61) as a sum of singular and regular parts, and denote them $F^s(t_x, \tau)$ and $F^r(t_x, \tau)$ respectively, that is

$$g_\alpha\left(\frac{h}{2}(t_x + 1)\psi_p\left(-\frac{1+\tau}{2}\right)\right) T_k(\psi_{p,L}(t_x, \tau))\psi'_{p,L}(t_x, \tau) = F^r(t_x, \tau) + F^s(t_x, \tau), \quad (66)$$

where

$$F^r(t_x, \tau) = \frac{h}{2} \left[\log\left(\frac{h}{2}\right) + \log\left|\frac{t_x + 1}{2^p} Q_p\left(-\frac{1+\tau}{2}\right)\right| \right] T_k(\psi_{p,L}(t_x, \tau)) \left(\frac{1+t_x}{2}\right) \psi'_p(\tau), \quad (67)$$

and

$$F^s(t_x, \tau) = \frac{h}{2} p \log(1 - \tau) T_k(\psi_{p,L}(t_x, \tau)) \left(\frac{1+t_x}{2}\right) \psi'_p(\tau). \quad (68)$$

Using (3) of Lemma(4.4), F^s can be factorized as $F^s(t_x, \tau) = f^s(\tau)\eta(t_x, \tau)$, where

$$\eta(t_x, \tau) = \frac{h}{2} \frac{p(t_x + 1)}{2^p} T_k(\psi_{p,L}(t_x, \tau)) R_p\left(-\frac{1+\tau}{2}\right), \quad f^s(\tau) = (1 - \tau)^{p-1} \log(1 - \tau).$$

Since Q_p, T_k and ψ_p are smooth, F^r is a smooth function and $\mathcal{K}_{ff}^n[F^r]$ converges super-algebraically to the integral of F^r using Theorem 3.8. Employing (5) of Lemma(4.4), η is a smooth function and doesn't contribute asymptotically to the singularity at $\tau = 1$ in f^s . Therefore, an application of [6, Theorem 6] for $f^s(\tau)$ we obtain the following estimate:

$$\left| \beta_{k,L}(x) - \tilde{\beta}_{k,L}(x) \right| \leq C \frac{h \log n_\beta}{n_\beta^{2p}}. \quad (69)$$

Similarly, to estimate the error in $|\beta_{k,R}(x) - \tilde{\beta}_{k,R}(x)|$ for $x \in \Omega \setminus \{b\}$, utilizing (2) of Lemma 4.4, one can decompose the integrand (62) as a sum of singular F^s and regular F^r part, from which we get $f^s(\tau) = (1 + \tau)^{p-1} \log(1 + \tau)$, whose integral is same as the integral of $(1 - \tau)^{p-1} \log(1 - \tau)$ on $[-1, 1]$. Therefore, one can derive exactly the same bound as $\beta_{k,R}$ in this case as well. \square

Remark 4.6. In the implementation of the method for the kernels with $0 < \alpha < 1$, the authors in [4] observed an interesting picture related to the order of convergence of the method. In particular, in [4], the authors numerically noticed that for kernels of the form $g_\alpha(x, y) = |x - y|^\alpha$, where $0 < \alpha < 1$, the method achieves high-order convergence (in terms of the regularity of u) if $p(1 - \alpha) \in \mathbb{N}$; otherwise it yields low order convergence.

Lemma 4.7. *Let $x \in \Omega$ and $g_\alpha(|x - y|) = |x - y|^{-\alpha}$, that is $0 < \alpha < 1$. Then, for $k \geq 0$*

$$\left| \beta_k(x) - \tilde{\beta}_k(x) \right| \leq C \begin{cases} \frac{h^{1-\alpha}}{n_\beta^\lambda}, & \text{if } p(1 - \alpha) \in \mathbb{N} \\ \frac{h^{1-\alpha}}{n_\beta^{2p(1-\alpha)}}, & \text{if } p(1 - \alpha) \notin \mathbb{N}, \end{cases} \quad (70)$$

where $p \geq 2$ is an integer, λ is any arbitrary positive integer, h is the length of patch the Ω , n_β denotes the number of quadrature nodes in the FF-Rule approximation both $\tilde{\beta}_{k,L}(x)$ and $\tilde{\beta}_{k,R}(x)$, and C is some constant independent of h and n_β .

Proof. We first estimate the error $|\beta_{k,L}(x) - \tilde{\beta}_{k,L}(x)|$ for $x \in \Omega \setminus \{a\}$. Utilizing (2),(3) of Lemma 4.4, decompose the integrand in (61) as a product of singular f^s and regular η part, that is

$$g_\alpha \left(\frac{h}{2}(t_x + 1)\psi_p \left(-\frac{1 + \tau}{2} \right) \right) T_k(\psi_{p,L}(t_x, \tau))\psi'_{p,L}(t_x, \tau) = f^s(\tau)\eta(t_x, \tau), \quad (71)$$

where

$$f^s(\tau) = (1 - \tau)^{p(1-\alpha)-1}, \quad \eta(t_x, \tau) = \left(\frac{h t_x + 1}{2} \frac{1}{2^p} \right)^{1-\alpha} \left| Q_p \left(-\frac{1 + \tau}{2} \right) \right|^{-\alpha} T_k(\psi_{p,L}(t_x, \tau)) R_p \left(-\frac{1 + \tau}{2} \right).$$

The analysis further can be divided into two cases: one where $p(1 - \alpha)$ is a natural number, and the other where it is not. In the first case $f^s(\tau)$ becomes a polynomial, which is smooth in $[-1, 1]$. From Theorem 3.8 it follows that FF-Rule converges super-algebraically for such functions. If $p(1 - \alpha)$ is not an integer, employing (5) of Lemma 4.4, η is a smooth function and doesn't contribute asymptotically to the singularity at $\tau = 1$ in f^s . Therefore, using [13, Theorem 1] for $f^s(\tau) = (1 - \tau)^\sigma$, with $\sigma = p(1 - \alpha) - 1$, we have the following estimate for $x \in \Omega \setminus \{a\}$

$$\left| \beta_{k,L}(x) - \tilde{\beta}_{k,L}(x) \right| \leq C \frac{h^{1-\alpha}}{n_\beta^{2p(1-\alpha)}}. \quad (72)$$

Similarly, we can show that $\left| \beta_{k,R}(x) - \tilde{\beta}_{k,R}(x) \right|$ satisfy the same estimate. \square

We now give an estimate for E_3^n (53) in the following theorem.

Theorem 4.8. *If $u \in X^m(\Omega)$ then*

$$E_3^n[u](x) \leq C \begin{cases} \frac{h \log n_\beta}{n_\beta^{2p}}, & \text{if } \alpha = 0 \\ \frac{h^{1-\alpha}}{n_\beta^\lambda}, & \text{if } 0 < \alpha < 1, p(1 - \alpha) \in \mathbb{N} \\ \frac{h^{1-\alpha}}{n_\beta^{2p(1-\alpha)}}, & \text{if } 0 < \alpha < 1, p(1 - \alpha) \notin \mathbb{N}, \end{cases} \quad (73)$$

where $p \geq 2$ is an integer, λ is any arbitrary positive integer, h is length of patch Ω , n_β denotes the number of quadrature nodes in the FF-Rule approximation of $\beta_{k,L}(x)$ and $\beta_{k,R}(x)$ (15), and C is some constant independent of h and n_β .

Proof. Using the definition of $E_3^n[u]$ in (53) and employing Lemma 4.5, and Lemma 4.7, the result follows. \square

4.3 Total error

In this section, we present the total error in the methodology discussed in 2. First we derive the total error for a single patch $\Omega = [a, b]$ where $h = b - a$ is a constant. In the later case, we derive the error in Ω with varying patches.

Theorem 4.9. (*Single Patch*) *If $u \in X^m[a, b]$ then the total error E_{tot}^n in the quadrature for a single patch is given by the following:*

1. For $\alpha = 0$,

$$E_{\text{tot}}^n[u](x) \leq C \left(\frac{(\log n)^2}{n^{m+2}} + \frac{\log n_\beta}{n_\beta^{2p}} \right). \quad (74)$$

2. For $0 < \alpha < 1$,

$$E_{\text{tot}}^n[u](x) \leq C \left(\frac{1}{n^{m+2-\alpha}} + \frac{1}{n_\beta^\lambda} \right), \text{ where } \lambda = \begin{cases} k, & \text{if } p(1-\alpha) \in \mathbb{N}, k \in \mathbb{N} \\ 2p(1-\alpha), & \text{if } p(1-\alpha) \notin \mathbb{N}, \end{cases} \quad (75)$$

p is the order of the change of variable used in the computation of $\tilde{\beta}_k(x)$, n is the number of terms in discrete Chebyshev expansion, n_β is the number of FF quadrature points used in the approximation of $\beta_k(x)$ (15), and C is some constant independent of n and n_β .

Proof. Proof follows from the error inequality (50), and ignoring h in Theorem 4.2, Theorem 4.3 and Theorem 4.8. \square

In the above theorem we have discussed error estimates for the singular quadrature on a single patch, now we derive the bounds in the case of varying patches.

Theorem 4.10. (*Varying Patches*) *Let P denote the number of patches of Ω with length of each patch bounded by $O(1/P)$. Let n and n_β denote the highest degree of the Chebyshev polynomial which approximates u (see (10)) and the number of quadrature points used in the approximation of $\beta_k^\ell(x)$ (see (16)) respectively. If $u \in X^m(\Omega)$, $g_\alpha(|x-y|)$ is as defined in equation (2), and $n > m+1$, then the total error in the proposed quadrature satisfies*

$$E_{\text{tot}}^n[u] = \max_{1 \leq \ell \leq P} E_{\ell, \text{sing}}^n[u] \quad (76)$$

where

1. For $\alpha = 0$,

$$E_{\ell, \text{sing}}^n[u] \leq C \left(\frac{h_\ell^{m+2} |\log h_\ell|}{n^{m+3}} + \frac{h_\ell^{m+2} (\log n)^2}{n^{m+2}} + \frac{h_\ell \log n_\beta}{n_\beta^{2p}} \right). \quad (77)$$

2. For $0 < \alpha < 1$,

$$E_{\ell, \text{sing}}^n[u] \leq C \left(\frac{h_\ell^{m+2-\alpha}}{n^{m+2-\alpha}} + \frac{h_\ell^{1-\alpha}}{n_\beta^\lambda} \right), \text{ where } \lambda = \begin{cases} k, & \text{if } p(1-\alpha) \in \mathbb{N}, k \in \mathbb{N} \\ 2p(1-\alpha), & \text{if } p(1-\alpha) \notin \mathbb{N}, \end{cases} \quad (78)$$

$p \geq 2$ is the order of the change of variable used in the computation of $\tilde{\beta}_k^\ell(x)$, and C is some constant independent of h_ℓ, n , and n_β .

Proof. Without loss of generality, assume that $x \in \Omega_\ell$ for some $\ell = 1, \dots, P$, that is, there is only one singular patch Ω_ℓ . The total error $E_{\text{tot}}^n[u](x)$ is the sum of the error in the singular integral $E_{\ell, \text{sing}}^n[u](x)$ (which is on Ω_ℓ) and errors in the regular integral $E_{\text{reg}}^n[u](x)$ (on other patches for $\Omega_j, j \neq \ell$). That is,

$$E_{\text{tot}}^n[u](x) \leq \left| \int_{\Omega_\ell} g_\alpha(|x-y|)u(y)dy - \mathcal{K}_{\ell, \text{sing}}^n[u](x) \right| + \sum_{\substack{j=1 \\ j \neq \ell}}^P \left| \int_{\Omega_j} g_\alpha(|x-y|)u(y)dy - \mathcal{K}_{j, \text{reg}}^n[u](x) \right|, \quad (79)$$

where $\mathcal{K}_{\ell, \text{sing}}^n[u](x)$ and $\mathcal{K}_{j, \text{reg}}^n[u](x)$ are the singular and regular integral approximations as defined in (16) and (8) respectively. Denoting the first and the second terms of (79) by the singular error $E_{\ell, \text{sing}}^n[u](x)$ and the regular error $E_{\text{reg}}^n[u](x)$ respectively, and employing Theorem 4.2, Theorem 4.3 and Theorem 4.8 with $h = h_\ell$, the error term $E_{\ell, \text{sing}}^n[u](x)$ for $0 < \alpha < 1$ becomes

$$E_{\ell, \text{sing}}^n[u](x) \leq C \left(\frac{h_\ell^{m+2-\alpha}}{n^{m+2-\alpha}} + \frac{h_\ell^{1-\alpha}}{n^\lambda} \right), \quad \text{where } \lambda = \begin{cases} k, & \text{if } p(1-\alpha) \in \mathbb{N}, k \in \mathbb{N} \\ 2p(1-\alpha), & \text{if } p(1-\alpha) \notin \mathbb{N}, \end{cases} \quad (80)$$

and for $\alpha = 0$ it becomes

$$E_{\ell, \text{sing}}^n[u](x) \leq C \left(\frac{h_\ell^{m+2} |\log h_\ell|}{n^{m+3}} + \frac{h_\ell^{m+2} (\log n)^2}{n^{m+2}} + \frac{h_\ell \log n_\beta}{n_\beta^{2p}} \right). \quad (81)$$

We now show that the error in regular integration $E_{\text{reg}}^n[u](x)$ will not contribute to the total error $E_{\text{tot}}^n[u]$. For the estimation of total regular error $E_{\text{reg}}^n[u](x)$, observe that $u \in X^m(\Omega)$, which implies there exists finitely many discontinuities of $u^{(m+2)}$ contained in finitely many patches, say n_d number of patches. Additionally, notice that $u \in C^{m+2}$ on $(P - n_d)$ patches, and using Theorem 3.8 the regular error $E_{\text{reg}}^n[u](x)$ can be written as

$$E_{\text{reg}}^n[u](x) = (P - n_d) O \left(\frac{h_{j_1}^{m+3}}{n^{m+2}} \right) + n_d O \left(\frac{h_{j_2}^{m+2}}{n^{m+2}} \right), \quad (82)$$

where $j_1, j_2 \in \{1, \dots, P\}$ such that j_1 and j_2 are the maximum length of the $(P - n_d)$ patches (where $u \in C^{m+2}$) and n_d patches (where $u^{(m)}$ is piecewise C^2). Since $h_j = O(1/P)$ for each j , and letting $h_{j_0} = \max\{h_{j_1}, h_{j_2}\}$, we obtain $E_{\text{reg}}^n[u](x) = O \left(h_{j_0}^{m+2} / n^{m+2} \right)$. Thus, the total error $E_{\text{tot}}^n[u](x)$ for $x \in \Omega_\ell$ becomes

$$E_{\text{tot}}^n[u] = E_{\ell, \text{sing}}^n[u] + O \left(\frac{h_{j_0}^{m+2}}{n^{m+2}} \right). \quad (83)$$

Since the total error in the proposed quadrature $E_{\text{tot}}^n[u]$ is the supremum of the total errors corresponding to each point x which is derived in (83) and observing the fact the patch length h_{j_0} corresponds to some $x' \in \Omega_{j_0}$, the total error is given by $E_{\text{tot}}^n[u] = \sup_{x \in \Omega} E_{\text{tot}}^n[u](x) = \max_{1 \leq \ell \leq P} E_{\ell, \text{sing}}^n[u]$ as desired. \square

Theorem 4.11. (*Varying Patches with uniform patch-length*) *If $u \in X^m(\Omega)$, $\Omega = [a, b]$ and $g_\alpha(|x-y|)$ is as defined in equation (2), then for any number of patches, total error in the proposed quadrature for $n > m+1$ is given by the following.*

1. For $\alpha = 0$,

$$E_{\text{tot}}^n[u] \leq C \left(\frac{h^{m+2} |\log h|}{n^{m+3}} + \frac{h^{m+2} (\log n)^2}{n^{m+2}} + \frac{h \log n_\beta}{n_\beta^{2p}} \right) \quad (84)$$

2. For $0 < \alpha < 1$,

$$E_{\text{tot}}^n[u] \leq C \left(\frac{h^{m+2-\alpha}}{n^{m+2-\alpha}} + \frac{h^{1-\alpha}}{n^\lambda} \right), \quad \text{where } \lambda = \begin{cases} k, & \text{if } p(1-\alpha) \in \mathbb{N}, k \in \mathbb{N} \\ 2p(1-\alpha), & \text{if } p(1-\alpha) \notin \mathbb{N}, \end{cases} \quad (85)$$

where h is the uniform length of the patches given by $h = \frac{b-a}{P}$, $p \geq 2$ is the order of the change of variable used in the computation of $\tilde{\beta}_k^l(x)$, n_β is the number of quadrature points used in the approximation of $\beta_k^l(x)$ (see (16)), n denotes the highest degree of the Chebyshev polynomial which approximates u (see (10)), and C is some constant independent of h_ℓ, n , and n_β .

Proof. Proof follows from Theorem 4.10. □

Remark 4.12. The error estimate for fixed number of patches (possibly more than one) is the same as error presented in Theorem 4.9, which is an immediate consequence of Theorem 4.10

5 Numerical results

This section presents the computational performance of the one-dimensional high-order integration scheme described in Section 2. The theoretical convergence rate presented in Theorem 4.9 and Theorem 4.11 is numerically demonstrated through a variety of numerical results, which are consistently in agreement with the theoretical order of convergence (toc). Throughout this section, we denote the number of nodes used in Chebyshev expansion of u in each patch by n , quadrature nodes in approximating singular integrals by n_β given by $n_\beta = 4n$, the total number of patches by P , the total number of grid points in the integration domain by N given by $N = n \times P$, p denotes the order of the change of variable ψ_p defined in equation (13), and the relative error denoted by $\epsilon_{N,\infty}$. The numerical order of convergence (noc) is computed using the formula

$$\text{noc} = \log_b \left(\frac{\epsilon_{N,\infty}}{\epsilon_{bN,\infty}} \right), \text{ where } \epsilon_{N,\infty} = \frac{\max_{1 \leq j \leq N} |u_j - u_j^{ex}|}{\max_{1 \leq j \leq N} |u_j^{ex}|},$$

and $b = 2, 3$. Here, u_j^{ex} denotes the exact solution corresponding to the approximated solution u_j at the quadrature point x_j . As elucidated in Section 2, there are two approaches to achieve the high-order convergence of the method: either by increasing the number of quadrature points in each patch while keeping the number of patches fixed or by increasing the number of patches (hence reducing the size of patches) but keeping the number of integration nodes in each patch fixed. Thus, in what follows, we present the convergence behavior for both approaches as mentioned above.

Example 5.1. Convergence illustration for the fixed patch case when $\alpha = 0$

Consider $g_\alpha(|x - y|) = \log|x - y|$, $u(y) = y^m|y|$ over the domain $\Omega = [-1, 1]$. As per Theorem 4.9, the rate of convergence of our method will be $\text{toc} = \min\{2p, m + 2\}$. For $m = 3, 4$ and $p = 2, 3, 4$ relative errors at various levels of discretization are presented in Table 2. In Table 2, one can see the effect of p on the noc for fixed regularity of the integral density u . To see the effect of the regularity parameter m of density u , we take $p = 5$ and approximate the integral (1) for various values of m . In Table 3, errors at various discretization levels are reported for the numerical approximation of (1) with $m = 0, 1, \dots, 6$, while keeping $p = 5$ in all the case. The Numerical order of convergence reported in these tables agrees with the theoretical order of convergence.

Example 5.2. Convergence illustration for the patches varying case when $\alpha = 0$

Consider $g_\alpha(x - y) = \ln|x - y|$ with two integral densities $u(y) = y^2|y| + 1$ and $u(y) = y^3|y|$. Table 4 presents the numerical results of this experiment for $p = 2$ and $p = 3$ with $n = 16$. One can see that, for the above mentioned u , the method yields only first-order convergence which is explained by Theorem 4.11. Specifically, if $u \in X^m$ and we choose p such that the term $\log(n)/n^{2p}$ is small in comparison to other error terms, then the method will yield order of convergence $m + 2$ demonstrated in Table 5 for $p = 4, 5$ and 6.

Example 5.3. Convergence illustration for fixed patch approach when $0 < \alpha < 1$

Consider the kernel $g_\alpha(x - y) = |x - y|^{-\alpha}$, $\alpha = 0.75, 0.9$ for $u(y) = y^3|y| \in X^3[-1, 1]$ and $u(y) = y^4|y| \in X^4[-1, 1]$ with $p = 2, 3, 6$. As per Theorem 4.9, the order of convergence of the method will rely

n	m=3						m=4					
	p=2, toc=4		p=3, toc=5		p=4, toc=5		p=2, toc=4		p=3, toc=6		p=4, toc=6	
	$\epsilon_{n,\infty}$	noc	$\epsilon_{n,\infty}$	noc	$\epsilon_{n,\infty}$	noc	$\epsilon_{n,\infty}$	noc	$\epsilon_{n,\infty}$	noc	$\epsilon_{n,\infty}$	noc
4	4.00e-02	-	4.44e-02	-	4.46e-02	-	1.06e-01	-	1.08e-01	-	9.88e-02	-
8	2.74e-04	7.19	2.75e-04	7.33	2.75e-04	7.34	3.41e-04	8.28	3.40e-04	8.31	3.40e-04	8.19
16	6.73e-06	5.35	6.73e-06	5.35	6.73e-06	5.35	8.01e-06	5.41	4.52e-06	6.23	4.52e-06	6.23
32	2.60e-07	4.70	1.99e-07	5.08	1.99e-07	5.08	4.85e-07	4.05	7.81e-08	5.85	7.81e-08	5.85
64	1.75e-08	3.89	6.14e-09	5.02	6.14e-09	5.02	3.03e-08	4.00	1.39e-09	5.81	1.39e-09	5.81
128	1.11e-09	3.98	1.91e-10	5.00	1.91e-10	5.00	1.90e-09	4.00	2.47e-11	5.82	2.47e-11	5.82
256	6.94e-11	4.00	5.98e-12	5.00	5.98e-12	5.00	1.19e-10	4.00	4.35e-13	5.83	4.33e-13	5.84
512	4.38e-12	3.98	1.87e-13	5.00	1.87e-13	5.00	7.49e-12	3.98	4.07e-14	3.42	5.50e-14	2.98
1024	3.50e-13	3.65	2.97e-14	2.66	2.39e-14	2.97	5.98e-13	3.65	-	-	-	-

Table 2: Convergence of the proposed integration scheme (fixed patch approach) to the approximation of integral operator (1) for the kernel $g_\alpha(x - y) = \log|x - y|$ with $u(y) = y^m|y|$.

n	m=0,toc=2		m=1,toc=3		m=2,toc=4		m=3,toc=5		m=4,toc=6		m=5,toc=7		m=6,toc=8	
	$\epsilon_{n,\infty}$	noc	$\epsilon_{n,\infty}$	noc	$\epsilon_{n,\infty}$	noc	$\epsilon_{n,\infty}$	noc	$\epsilon_{n,\infty}$	noc	$\epsilon_{n,\infty}$	noc	$\epsilon_{n,\infty}$	noc
4	8.74e-02	-	3.15e-02	-	3.93e-02	-	2.88e-02	-	6.98e-02	-	1.03e-01	-	1.18e-01	-
8	2.99e-02	1.55	1.23e-03	4.68	1.71e-03	4.52	2.76e-04	6.70	3.39e-04	7.69	1.59e-04	9.34	9.21e-04	7.00
16	9.77e-03	1.61	1.43e-04	3.10	1.27e-04	3.76	6.73e-06	5.36	4.52e-06	6.23	6.55e-07	7.92	3.57e-07	11.3
32	3.07e-03	1.67	1.77e-05	3.01	9.67e-06	3.71	1.99e-07	5.08	7.81e-08	5.85	4.51e-09	7.18	1.35e-09	8.05
64	9.30e-04	1.72	2.21e-06	3.01	7.16e-07	3.76	6.14e-09	5.02	1.39e-09	5.81	3.41e-11	7.04	5.71e-12	7.89
128	2.74e-04	1.77	2.76e-07	3.00	5.19e-08	3.79	1.91e-10	5.00	2.47e-11	5.82	2.65e-13	7.01	1.80e-13	4.99
256	7.87e-05	1.80	3.45e-08	3.00	3.70e-09	3.81	5.98e-12	5.00	4.34e-13	5.83	4.37e-14	2.60	1.38e-13	0.38
512	2.22e-05	1.82	4.31e-09	3.00	2.59e-10	3.83	1.87e-13	5.00	4.07e-14	3.41	-	-	-	-
1024	6.20e-06	1.84	5.38e-10	3.00	1.80e-11	3.85	2.27e-14	3.04	-	-	-	-	-	-

Table 3: Convergence of the proposed integration scheme (fixed patch approach) to the approximation of integral operator (1) for the kernel $g_\alpha(x - y) = \log|x - y|$ with $u(y) = y^m|y|$, $m = 0, 1, \dots, 6$, and $p = 5$.

$P \times n$	m=2				m=3			
	p=2, toc=1		p=3, toc=1		p=2, toc=1		p=3, toc=1	
	$\epsilon_{N,\infty}$	noc	$\epsilon_{N,\infty}$	noc	$\epsilon_{N,\infty}$	noc	$\epsilon_{N,\infty}$	noc
1×16	4.03e-04	-	4.03e-04	-	2.74e-04	-	2.74e-04	-
3×16	7.18e-06	3.67	7.15e-06	3.67	1.08e-06	5.04	1.08e-06	5.04
9×16	1.25e-07	3.69	1.15e-07	3.76	3.14e-08	3.22	4.44e-09	5.00
27×16	6.53e-09	2.69	1.74e-09	3.82	1.05e-08	1.00	7.16e-11	3.76
81×16	2.18e-09	1.00	1.85e-11	4.41	3.51e-09	1.00	2.39e-11	1.00
243×16	7.26e-10	1.00	4.95e-12	1.20	1.17e-09	1.00	7.97e-12	1.00
729×16	2.42e-10	1.00	1.65e-12	1.00	3.90e-10	1.00	2.66e-12	1.00
2187×16	8.06e-11	1.00	5.53e-13	0.99	1.30e-10	1.00	8.90e-13	1.00

Table 4: Convergence of the proposed integration scheme (varying patch approach) to the approximation of integral operator (1) for the kernel $g_\alpha(x - y) = \log|x - y|$ with the integral densities $u(y) = y^m|y| + 1$ ($m = 2$) and $u(y) = y^m|y|$ ($m = 3$).

upon three parameters α , m , and p . To be precise, if $p(1 - \alpha) \in \mathbb{N}$ then $\text{toc} = m + 2 - \alpha$, otherwise $\text{toc} = \min\{m + 2 - \alpha, 2p(1 - \alpha)\}$.

For $p = 2, 3, 6$, the term $p(1 - \alpha) \notin \mathbb{N}$, therefore in this case $\text{toc} = \min\{m + 2 - \alpha, 2p(1 - \alpha)\}$. Since $2p(1 - \alpha) < m + 2 - \alpha$ for $m = 3, 4$ and $p = 2, 3, 6$ with $\alpha = 0.75, 0.9$, the toc is dominated by the quantity $2p(1 - \alpha)$, which is exactly demonstrated numerically in Table 6 and Table 7 for $m = 3$ and $m = 4$ respectively.

Therefore, in this case to achieve optimal order of convergence in terms of m , the choices of the order of change of variable p for $\alpha = 0.75$ are $p \in 4\mathbb{N}$ and for $\alpha = 0.9$ are $p \in 10\mathbb{N}$. For instance, if $m = 3$ then the toc is 4.25 and 4.10 for $\alpha = 0.75$ and $\alpha = 0.9$ respectively. We numerically describe this behavior of

$P \times n$	m=2						m=3					
	p=4, toc=4		p=5, toc=4		p=6, toc=4		p=4, toc=5		p=5, toc=5		p=6, toc=5	
	$\epsilon_{n,\infty}$	noc	$\epsilon_{n,\infty}$	noc	$\epsilon_{n,\infty}$	noc	$\epsilon_{n,\infty}$	noc	$\epsilon_{n,\infty}$	noc	$\epsilon_{n,\infty}$	noc
1×16	4.03e-04	-	4.03e-04	-	4.03e-04	-	2.74e-04	-	2.74e-04	-	2.74e-04	-
3×16	7.15e-06	3.67	7.15e-06	3.67	7.15e-06	3.67	1.08e-06	5.04	1.08e-06	5.04	1.08e-06	5.04
9×16	1.15e-07	3.76	1.15e-07	3.76	1.15e-07	3.76	4.44e-09	5.00	4.44e-09	5.00	4.44e-09	5.00
27×16	1.76e-09	3.81	1.76e-09	3.81	1.76e-09	3.81	1.82e-11	5.00	1.82e-11	5.00	1.82e-11	5.00
81×16	2.60e-11	3.84	2.59e-11	3.84	2.59e-11	3.84	1.85e-13	4.18	7.49e-14	5.00	7.49e-14	5.00
243×16	3.91e-13	3.82	3.72e-13	3.86	3.72e-13	3.86	6.17e-14	1.00	3.20e-15	2.87	2.70e-15	3.03
729×16	3.12e-14	2.30	6.27e-15	3.72	6.48e-15	3.69	2.24e-14	0.92	-	-	-	-
2187×16	1.65e-14	0.58	-	-	-	-	1.25e-14	0.53	-	-	-	-

Table 5: Convergence of the proposed integration scheme (varying patch approach) to the approximation of integral operator (1) for the kernel $g_\alpha(x - y) = \log|x - y|$ with the integral densities $u(y) = y^m|y| + 1$ ($m = 2$) and $u(y) = y^m|y|$ ($m = 3$). Increasing the value of p leads to a high-order convergence rate.

n	$\alpha = 0.75, u(y) = y^3 y $						$\alpha = 0.9, u(y) = y^3 y $					
	p=2, toc=1		p=3, toc=1.5		p=6, toc=3		p=2, toc=0.4		p=3, toc=0.6		p=6, toc=1.2	
	$\epsilon_{n,\infty}$	noc	$\epsilon_{n,\infty}$	noc	$\epsilon_{n,\infty}$	noc	$\epsilon_{n,\infty}$	noc	$\epsilon_{n,\infty}$	noc	$\epsilon_{n,\infty}$	noc
4	5.18e-02	-	6.12e-03	-	1.28e-02	-	3.48e-01	-	2.01e-01	-	1.93e-02	-
8	2.92e-02	0.83	1.87e-03	1.71	1.29e-03	3.32	2.71e-01	0.36	1.39e-01	0.53	1.10e-02	0.80
16	1.47e-02	0.99	7.14e-04	1.39	5.22e-05	4.62	2.08e-01	0.38	9.26e-02	0.58	4.87e-03	1.18
32	7.37e-03	0.99	2.55e-04	1.48	6.15e-06	3.08	1.57e-01	0.41	6.08e-02	0.61	2.11e-03	1.21
64	3.69e-03	1.00	9.04e-05	1.50	7.63e-07	3.01	1.19e-01	0.40	4.02e-02	0.60	9.21e-04	1.20
128	1.84e-03	1.00	3.20e-05	1.50	9.52e-08	3.00	9.01e-02	0.40	2.65e-02	0.60	4.01e-04	1.20
256	9.22e-04	1.00	1.13e-05	1.50	1.19e-08	3.00	6.83e-02	0.40	1.75e-02	0.60	1.74e-04	1.20
512	4.61e-04	1.00	4.00e-06	1.50	1.49e-09	3.00	5.17e-02	0.40	1.15e-02	0.60	7.59e-05	1.20
1024	2.30e-04	1.00	1.41e-06	1.50	1.86e-10	3.00	3.92e-02	0.40	7.60e-03	0.60	3.30e-05	1.20

Table 6: Convergence of the proposed integration scheme (fixed patch approach with $P = 1$) to the approximation of integral operator (1) for the kernel $g_\alpha(x - y) = |x - y|^{-\alpha}$, $\alpha = 0.75, 0.9$ with $u(y) = y^3|y|$.

n	$\alpha = 0.75, u(y) = y^4 y $						$\alpha = 0.9, u(y) = y^4 y $					
	p=2, toc=1		p=3, toc=1.5		p=6, toc=3		p=2, toc=0.4		p=3, toc=0.6		p=6, toc=1.2	
	$\epsilon_{n,\infty}$	noc	$\epsilon_{n,\infty}$	noc	$\epsilon_{n,\infty}$	noc	$\epsilon_{n,\infty}$	noc	$\epsilon_{n,\infty}$	noc	$\epsilon_{n,\infty}$	noc
4	1.86e-02	-	2.91e-02	-	7.72e-03	-	3.33e-01	-	1.89e-01	-	1.68e-02	-
8	2.83e-02	-0.61	2.00e-03	3.86	2.46e-04	4.97	2.70e-01	0.30	1.38e-01	0.46	1.07e-02	0.65
16	1.46e-02	0.95	7.13e-04	1.49	5.05e-05	2.28	2.07e-01	0.38	9.23e-02	0.58	4.85e-03	1.14
32	7.22e-03	1.02	2.50e-04	1.51	5.97e-06	3.08	1.56e-01	0.41	6.05e-02	0.61	2.10e-03	1.21
64	3.59e-03	1.01	8.80e-05	1.51	7.41e-07	3.01	1.19e-01	0.39	4.00e-02	0.59	9.18e-04	1.19
128	1.79e-03	1.00	3.11e-05	1.50	9.26e-08	3.00	8.98e-02	0.40	2.64e-02	0.60	3.99e-04	1.20
256	8.97e-04	1.00	1.10e-05	1.50	1.16e-08	3.00	6.81e-02	0.40	1.74e-02	0.60	1.74e-04	1.20
512	4.49e-04	1.00	3.90e-06	1.50	1.45e-09	3.00	5.16e-02	0.40	1.15e-02	0.60	7.57e-05	1.20
1024	2.24e-04	1.00	1.38e-06	1.50	1.81e-10	3.00	3.91e-02	0.40	7.58e-03	0.60	3.29e-05	1.20

Table 7: Convergence of the proposed integration scheme (fixed patch approach) to the approximation of integral operator (1) for the kernel $g_\alpha(x - y) = |x - y|^{-\alpha}$, $\alpha = 0.75, 0.9$ with $u(y) = y^4|y|$.

the proposed method in Table 8. Similar behavior is noticed if $m = 4$ for $\alpha = 0.75$ and $\alpha = 0.9$ in Table 9.

Example 5.4. Convergence illustration for varying patch approach when $0 < \alpha < 1$

Consider the kernel $g_\alpha(x - y) = |x - y|^{-\alpha}$, $\alpha = 0.75$ and $u(y) = y^4|y| + y + 1 \in X^4[-1, 1]$. According to Theorem 4.11, if $p(1 - \alpha)$ is not an integer, then the toc is $1 - \alpha = 0.25$, which indicates poor convergence. For instance, if $p = 3, 5, 6, 7$, then the toc becomes 0.25, which is consistent with the numerical experiment shown in Table 10. However, if $p(1 - \alpha)$ is an integer, then the toc depends on the regularity of u which is $\text{toc} = m + 2 - \alpha$ as analytically estimated in Theorem 4.11. This phenomenon can be observed in the

n	$\alpha = 0.75, u(y) = y^3 y $						$\alpha = 0.9, u(y) = y^3 y $					
	p=4, toc=4.25		p=8, toc=4.25		p=12, toc=4.25		p=10, toc=4.10		p=20, toc=4.10		p=30, toc=4.10	
	$\epsilon_{n,\infty}$	noc	$\epsilon_{n,\infty}$	noc	$\epsilon_{n,\infty}$	noc	$\epsilon_{n,\infty}$	noc	$\epsilon_{n,\infty}$	noc	$\epsilon_{n,\infty}$	noc
4	1.54e-02	-	6.04e-02	-	1.72e-01	-	2.82e-02	-	8.43e-02	-	7.71e-02	-
8	1.54e-04	6.64	5.02e-03	3.59	5.08e-03	5.08	2.47e-03	3.51	9.02e-03	3.23	1.42e-02	2.44
16	4.64e-06	5.06	3.32e-05	7.24	5.35e-05	6.57	1.71e-05	7.18	2.01e-05	8.81	5.18e-05	8.10
32	2.27e-07	4.35	5.07e-07	6.03	1.61e-06	5.06	3.77e-07	5.50	6.59e-07	4.93	1.31e-06	5.30
64	1.18e-08	4.27	2.62e-08	4.27	4.57e-08	5.14	9.55e-09	5.30	2.45e-08	4.75	3.86e-08	5.09
128	6.17e-10	4.25	6.93e-10	5.24	1.44e-09	4.98	3.61e-10	4.73	8.28e-10	4.89	1.25e-09	4.94
256	3.24e-11	4.25	3.24e-11	4.42	6.13e-11	4.56	2.10e-11	4.10	2.47e-11	5.06	3.96e-11	4.99
512	1.70e-12	4.25	1.70e-12	4.25	1.95e-12	4.98	1.23e-12	4.10	1.23e-12	4.34	1.24e-12	4.99
1024	1.68e-13	3.34	1.79e-13	3.25	2.14e-13	3.18	2.45e-13	2.32	2.20e-13	2.48	2.05e-13	2.60

Table 8: Convergence of the proposed integration scheme (fixed patch approach) to the approximation of integral operator (1) for the kernel $g_\alpha(x - y) = |x - y|^{-\alpha}$, $\alpha = 0.75, 0.9$ with $u(y) = y^3|y|$.

n	$\alpha = 0.75, u(y) = y^4 y $						$\alpha = 0.9, u(y) = y^4 y $					
	p=4, toc=5.25		p=8, toc=5.25		p=12, toc=5.25		p=10, toc=5.10		p=20, toc=5.10		p=30, toc=5.10	
	$\epsilon_{n,\infty}$	noc	$\epsilon_{n,\infty}$	noc	$\epsilon_{n,\infty}$	noc	$\epsilon_{n,\infty}$	noc	$\epsilon_{n,\infty}$	noc	$\epsilon_{n,\infty}$	noc
4	3.17e-02	-	4.29e-02	-	1.21e-01	-	2.21e-02	-	5.02e-02	-	2.64e-02	-
8	1.21e-04	8.04	4.41e-03	3.28	1.03e-02	3.56	2.96e-03	2.90	8.07e-03	2.64	1.92e-02	0.46
16	1.43e-06	6.40	1.66e-06	11.4	1.74e-05	9.20	2.75e-06	10.1	1.39e-05	9.18	2.41e-04	6.32
32	3.47e-08	5.37	3.47e-08	5.58	1.36e-07	7.01	2.15e-08	7.00	1.18e-07	6.88	3.07e-07	9.62
64	8.95e-10	5.28	8.95e-10	5.28	1.92e-09	6.14	4.47e-10	5.59	1.88e-09	5.97	3.94e-09	6.29
128	2.34e-11	5.26	2.34e-11	5.26	2.64e-11	6.18	1.30e-11	5.11	2.93e-11	6.00	6.35e-11	5.95
256	6.15e-13	5.25	6.14e-13	5.25	6.15e-13	5.43	3.78e-13	5.10	4.54e-13	6.01	9.89e-13	6.00
512	5.83e-14	3.40	5.79e-14	3.41	5.24e-14	3.55	7.03e-14	2.43	6.54e-14	2.79	8.17e-14	3.60

Table 9: Convergence of the proposed integration scheme (fixed patch approach) to the approximation of integral operator (1) for the kernel $g_\alpha(x - y) = |x - y|^{-\alpha}$, $\alpha = 0.75, 0.9$ with $u(y) = y^4|y|$.

same table when $p = 4, 8$, where the noc matches exactly with the toc.

P	p=4(toc=5.25)		p=5(toc=0.25)		p=6(toc=0.25)		p=7(toc=0.25)		p=8(toc=5.25)	
	ϵ_∞	noc	ϵ_∞	noc	ϵ_∞	noc	ϵ_∞	noc	ϵ_∞	noc
1	5.40e-05	-	5.72e-05	-	5.51e-05	-	5.41e-05	-	5.40e-05	-
3	1.47e-07	5.37	3.28e-06	2.60	1.17e-06	3.51	2.36e-07	4.95	1.47e-07	5.37
9	3.83e-10	5.42	2.66e-06	0.19	9.50e-07	0.19	1.52e-07	0.40	3.83e-10	5.42
27	1.13e-12	5.30	2.19e-06	0.18	7.82e-07	0.18	1.25e-07	0.18	1.13e-12	5.30
81	6.00e-15	4.77	1.80e-06	0.18	6.42e-07	0.18	1.03e-07	0.18	5.69e-15	4.82
243	-	-	1.46e-06	0.19	5.19e-07	0.19	8.29e-08	0.19	-	-
729	-	-	1.17e-06	0.20	4.17e-07	0.20	6.65e-08	0.20	-	-
2187	-	-	9.27e-07	0.21	3.31e-07	0.21	5.28e-08	0.21	-	-

Table 10: Convergence of the proposed integration scheme (varying patch approach) to the approximation of integral operator (1) for the kernel $g_\alpha(x - y) = |x - y|^{-\alpha}$, $\alpha = 0.75$ with $u(y) = y^4|y| + y + 1$.

6 Applications to surface scattering problem

The scattered wave u^s which arises in the acoustic scattering by sound soft obstacle Ω , is given by the unique solution of the following PDE.

$$\begin{cases} \Delta u^s(\mathbf{x}) + \kappa^2 u^s(\mathbf{x}) &= 0, & \mathbf{x} \in \mathbb{R}^2 \setminus \Omega, \\ u^s(\mathbf{x}) &= -u^i(\mathbf{x}), & \mathbf{x} \in \partial\Omega, \\ \lim_{r \rightarrow \infty} \sqrt{r} \left(\frac{\partial u^s}{\partial r} - i\kappa u^s \right) &= 0, \end{cases} \quad (86)$$

where u^i is the incident wave, κ is the wave number, $\Omega \subset \mathbb{R}^2$ is a bounded domain, $\partial\Omega$ the boundary of Ω , $r = \|\mathbf{x}\|$ and $i = \sqrt{-1}$. The obstacle Ω is of class C^2 and the fact, scattered wave satisfies the Sommerfeld radiation condition guarantee the existence of the unique solution to the above problem (86) whenever the wavenumber κ is positive [5]. An equivalent integral equation formulation of the above exterior Helmholtz problem in terms of the acoustic single and double layer potentials is given by

$$u^s(\mathbf{x}) = \int_{\partial\Omega} \left[\frac{\partial g_\kappa(\mathbf{x}, \mathbf{y})}{\partial \nu(\mathbf{y})} - i\eta g_\kappa(\mathbf{x}, \mathbf{y}) \right] \varphi(y), \quad \mathbf{x} \in \mathbb{R}^2 \setminus \Omega, \quad (87)$$

where the density φ is the solution of the following integral equation of the second kind

$$\frac{\varphi}{2} + (K\varphi)(\mathbf{x}) - i\eta(S\varphi)(\mathbf{x}) = u^i(\mathbf{x}), \quad \mathbf{x} \in \partial\Omega, \quad (88)$$

and $(S\varphi)(\mathbf{x}), (K\varphi)(\mathbf{x})$ are the acoustic single and double layer potentials defined as follows.

$$(S\varphi)(\mathbf{x}) = \int_{\partial\Omega} g_\kappa(\mathbf{x}, \mathbf{y}) \varphi(\mathbf{y}) ds(\mathbf{y}), \quad \text{and} \quad (K\varphi)(\mathbf{x}) = \int_{\partial\Omega} \frac{\partial g_\kappa(\mathbf{x}, \mathbf{y})}{\partial \nu(\mathbf{y})} \varphi(\mathbf{y}) ds(\mathbf{y}),$$

where $g_\kappa(\mathbf{x}, \mathbf{y}) = \frac{i}{4} H_0^1(\kappa|\mathbf{x} - \mathbf{y}|)$ is the Green function for the free space Helmholtz problem (86), ν is the unit normal vector directed to the exterior of Ω , and η is called the coupling constant. We illustrate the numerical solution of the problem discussed in (86) through the following experiments. The numerical results presented in this section were produced by means of a C++ implementation of the algorithms described in Section 2 on a single core of an Intel i7-11390H processor.

Example 6.1. In this example, we compute the numerical solution of the impenetrable scattering problem (87)-(88) on a circular region by considering a plane wave incidence. The method proposed in Section 2 can effectively solve large-scale problems without suffering from dispersion error. Numerical results for large wavenumbers are computed and presented in Table 11. In this table, the acronym ‘‘iter’’ denotes the number of GMRES iterations required to reach the GMRES tolerance 10^{-10} , it also illustrates the dispersion-free nature, as the solver’s accuracy does not deteriorate with the increase in wavenumber if the number of points per wavelength is maintained.

$P \times n$	κ	Points per λ	$\epsilon_{N,\infty}$	iter	Time (in seconds)		
					per iter	pre-comput	Total
8×15	10	12	8.09e-07	16	0.0006	0.005	0.03
16×15	20	12	2.09e-07	21	0.001	0.02	0.08
32×15	40	12	4.66e-08	26	0.004	0.06	0.24
64×15	80	12	5.74e-08	30	0.01	0.24	0.79
128×15	160	12	6.58e-08	35	0.05	0.98	3
256×15	320	12	6.86e-08	43	0.20	3.84	13
512×15	640	12	7.33e-08	52	0.74	15.07	57
1024×15	1280	12	4.62e-08	64	2.90	60.08	257
2048×15	2560	12	7.71e-08	79	-	-	-

Table 11: Performance of the solver for high wave numbers: Eight-digit accuracy is maintained using 12 points per wavelength. The GMRES tolerance is set to be 10^{-10} for all the results.

Example 6.2. This experiment illustrates the high-order convergence of our numerical integration scheme for star-shaped boundary. The parametrization of $\partial\Omega$ is

$$c(t) = r(t)(\cos t, \sin t), \quad r(t) = 1 + 0.3 \cos(5t), \quad 0 \leq t \leq 2\pi. \quad (89)$$

For the plane wave incidence with $\kappa = 12$, we compared our numerical solution with the reference solution computed at 21×21 equispaced grids on $[-3, 3]^2$. For computing the reference solution, consider $n = 20$ on each of the 512 patches. An iterative solver GMRES took 26 iterations with 10^{-14} tolerance to compute the reference solution at finer grids. The high-order convergence in both the approaches, patches fixed and patches varying, is attained and demonstrated in Table 12, respectively. In Figure 2, we display the surface scattering by star-shaped boundary when the incoming plane wave impinges on the obstacle from the positive x-axis with $\kappa = 40$.

$P \times n$	$\epsilon_{N,\infty}$	noc	time(in seconds)
1×15	1.77e+00	-	-
2×15	1.00+e00	0.82	0.01
4×15	1.40e-01	2.84	0.02
8×15	1.36e-02	3.36	0.06
16×15	7.21e-04	4.24	0.14
32×15	8.46e-07	9.73	0.38
64×15	4.48e-09	7.56	1.24
128×15	4.27e-13	13.36	4.39

$P \times n$	$\epsilon_{N,\infty}$	noc	time(in seconds)
5×4	5.29e+00	-	-
5×8	4.89e-01	3.44	0.01
5×16	4.77e-02	3.36	0.02
5×32	1.31e-03	5.18	0.07
5×64	1.49e-05	6.45	0.26
5×128	5.83e-10	14.65	1.18
5×256	1.99e-11	4.86	6.44
5×512	3.51e-12	2.51	39.92

Table 12: Illustration of high-order convergence of the proposed algorithm for the surface scattering by star-shaped scatterer with $\kappa = 12$.

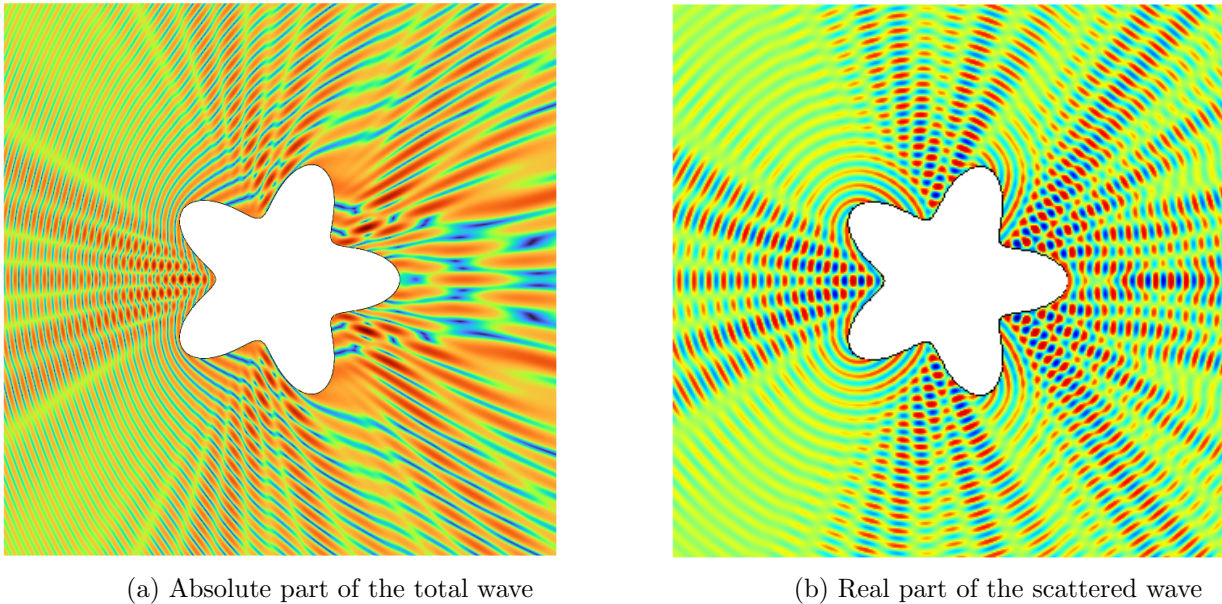


Figure 2: Illustration of the plane wave scattering by boundary of star shaped region for wavenumber $\kappa = 48$.

Example 6.3. The parametrization of $\partial\Omega$ is

$$c(t) = r(t)(\cos t, \sin t), \quad r(t) = 1 + 0.3 \cos(4t + 2 \sin t), \quad 0 \leq t \leq 2\pi.$$

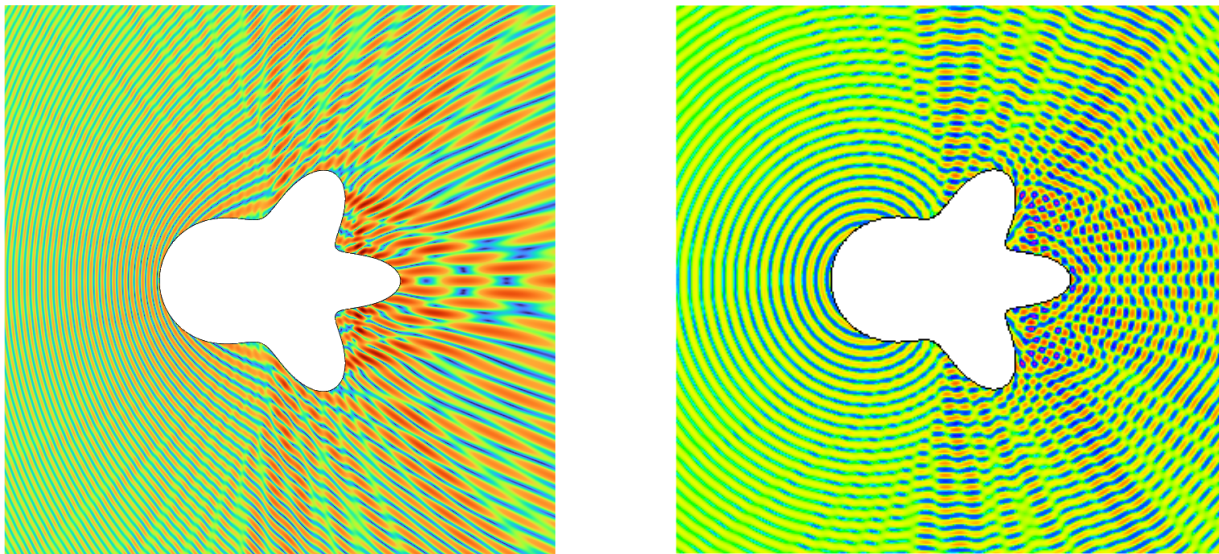
For the plane wave incidence with $\kappa = 10$, we compared our numerical solution with the reference solution computed at 21×21 equispaced grids on $[-3, 3]^2$. To compute the reference solution, we decomposed the jellyfish-shaped boundary into $P = 512$ patches and considered $n = 15$ on each patch. The GMRES took 23 iterations with 10^{-13} tolerance for the computation of reference solution. In Table 13, we display the high-order convergence in both the approaches, patches fixed and patches varying. Figure 3, shows the

$P \times n$	$\epsilon_{N,\infty}$	noc	time(in seconds)
4×15	1.16e-01	2.20	0.02
8×15	4.02e-03	4.85	0.06
16×15	1.77e-04	4.51	0.15
32×15	6.75e-08	11.4	0.41
64×15	2.14e-10	8.30	1.26
128×15	1.37e-13	10.6	4.28
256×15	4.70e-14	1.54	15.50

$P \times n$	$\epsilon_{N,\infty}$	noc	time(in seconds)
10×4	7.46 e-01	-	-
10×8	5.63e-02	3.73	0.02
10×16	1.24e-03	5.50	0.05
10×32	2.43e-06	9.00	0.17
10×64	2.34e-10	13.3	0.76
10×128	1.37e-13	10.7	3.61
10×256	9.63e-14	0.51	20.8

Table 13: Illustration of high-order convergence of the proposed algorithm for the surface scattering by jellyfish-shaped scatterer with $\kappa = 10$.

surface scattering by jellyfish-shaped boundary when the incoming plane wave impinges on the obstacle from the positive x-axis with $\kappa = 50$.



(a) Absolute value of the total wave

(b) Real part of the scattered wave

Figure 3: Illustration of the plane wave scattering by boundary of jellyfish shaped region for wavenumber $\kappa = 50$.

7 Conclusions

We have presented an efficient high-order integration scheme for evaluating singular integral in one dimension. The proposed method is very accurate and can achieve machine accuracy with fewer integration nodes. We have established a complete quadrature analysis of the proposed integration scheme and verified the theoretical convergence rate through several computational results. The novel aspects of this contribution are the classification of all degrees of PCV (used in the analytical resolution of kernel singularity) that can provide high-order convergence of the method and establishing a decay estimate on the continuous Chebyshev coefficients of integral density concerning its degree of smoothness and length of the domain. As an application of the method, we have employed the proposed scheme in conjunction with matrix-free iterative solver GMRES to solve impenetrable wave scattering by acoustic waves. In scattering simulations, the method's performance for large-scale problems is demonstrated through a variety of numerical results, and high-order convergence is obtained for a several complex domains.

8 Acknowledgements

Krishna acknowledges the financial support from CSIR through the file no. 09/1020(0183)/2019-EMR-I.

References

- [1] T. M. Apostol. *Introduction to analytic number theory*. Springer Science & Business Media, 2013.
- [2] O. P. Bruno and E. Garza. A Chebyshev-based rectangular-polar integral solver for scattering by geometries described by non-overlapping patches. *Journal of Computational Physics*, 421:109740, 2020.
- [3] O. P. Bruno and A. Pandey. Direct/iterative hybrid solver for scattering by inhomogeneous media. *SIAM Journal on Scientific Computing*, 46(2):A1298–A1326, 2024.
- [4] O. P. Bruno and S. Sachan. A fractional Laplacian weakly singular integral solver. in preparation.
- [5] D. Colton and R. Kress. *Integral equation methods in scattering theory*. SIAM, 2013.
- [6] G. Criscuolo, G. Mastroianni, and G. Monegato. Convergence properties of a class of product formulas for weakly singular integral equations. *Math. Comp.*, 55(191):213–230, 1990.
- [7] P. J. Davis and P. Rabinowitz. *Methods of Numerical Integration*. Academic Press, 2014.
- [8] V. Domínguez, I. G. Graham, and T. Kim. Filon–Clenshaw–Curtis rules for highly oscillatory integrals with algebraic singularities and stationary points. *SIAM Journal on Numerical Analysis*, 51(3):1542–1566, 2013.
- [9] L. M. Faria, C. Pérez-Arancibia, and M. Bonnet. General-purpose kernel regularization of boundary integral equations via density interpolation. *Computer Methods in Applied Mechanics and Engineering*, 378:113703, 2021.
- [10] E. Garza and C. Sideris. Fast inverse design of 3d nanophotonic devices using boundary integral methods. *ACS Photonics*, 10(4):824–835, 2022.
- [11] J. Hu, E. Garza, and C. Sideris. A Chebyshev-based high-order-accurate integral equation solver for Maxwell’s equations. *IEEE Transactions on Antennas and Propagation*, 69(9):5790–5800, 2021.
- [12] R. Kress. A Nyström method for boundary integral equations in domains with corners. *Numerische Mathematik*, 58(1):145–161, 1990.
- [13] M. Kütz. Asymptotic error bounds for a class of interpolatory quadratures. *SIAM journal on numerical analysis*, 21(1):167–175, 1984.
- [14] P.-G. Martinsson and V. Rokhlin. An accelerated kernel-independent fast multipole method in one dimension. *SIAM Journal on Scientific Computing*, 29(3):1160–1178, 2007.
- [15] J. C. Mason and D. C. Handscomb. *Chebyshev polynomials*. CRC press, 2002.
- [16] J. Ng. Acoustic waveform optimization for three-dimensional object geometries. 2023.
- [17] L. N. Trefethen. Is Gauss quadrature better than Clenshaw–Curtis? *SIAM review*, 50(1):67–87, 2008.
- [18] S. Xiang. On convergence rates of Fejér and Gauss–Chebyshev quadrature rules. *Journal of Mathematical Analysis and Applications*, 405(2):687–699, 2013.

- [19] S. Xiang, X. Chen, and H. Wang. Error bounds for approximation in Chebyshev points. *Numerische Mathematik*, 116(3):463–491, 2010.
- [20] S. Xiang, G. He, and Y. J. Cho. On error bounds of Filon-Clenshaw-Curtis quadrature for highly oscillatory integrals. *Advances in Computational Mathematics*, 41:573–597, 2015.
- [21] L. Zhang, L. Xu, and T. Yin. On the hyper-singular boundary integral equation methods for dynamic poroelasticity: three dimensional case. *arXiv preprint arXiv:2202.04257*, 2022.
- [22] Y. Zhang, C. Zhuang, and S. Jiang. Fast one-dimensional convolution with general kernels using sum-of-exponential approximation. *Communications in Computational Physics*, 29(5):1570–1582, 2021.